
CASA-B: A Unified Framework of Model-Free Reinforcement Learning

Changnan Xiao

ByteDance
xiaochangnan@bytedance.com

Haosen Shi

Nankai University
shihaosen98@gmail.com

Jiajun Fan

Nankai University
jiajunfanthu@gmail.com

Shihong Deng

ByteDance
dengshihong@bytedance.com

Abstract

Building on the breakthrough of reinforcement learning, this paper introduces a unified framework of model-free reinforcement learning, CASA-B, Critic AS an Actor with Bandits Vote Algorithm. CASA-B is an actor-critic framework that estimates state-value, state-action-value and policy. An expectation-correct Doubly Robust Trace is introduced to learn state-value and state-action-value, whose convergence properties are guaranteed. We prove that CASA-B integrates a consistent path for the policy evaluation and the policy improvement. The policy evaluation is equivalent to a compensational policy improvement, which alleviates the function approximation error, and is also equivalent to an entropy-regularized policy improvement, which prevents the policy from collapsing to a suboptimal solution. Building on this design, we find the entropy of the behavior policies' and the target policy's are disentangled. Based on this observation, we propose a progressive closed-form entropy control mechanism, which explicitly controls the behavior policies' entropy to arbitrary range. Our experiments show that CASA-B is super sample efficient and achieves State-Of-The-Art on Arcade Learning Environment. Our mean Human Normalized Score is 6456.63% and our median Human Normalized Score is 477.17%, under 200M training scale.

1 INTRODUCTION

Model-free reinforcement learning (MFRL) has made many impressive breakthroughs in a wide range of Markov decision processes (MDP) (Vinyals et al., 2019; Pedersen, 2019; Badia et al., 2020a). MFRL mainly consists of two categories, valued-based methods (Mnih et al., 2015; Hessel et al., 2017) and policy-based methods (Schulman et al., 2015, 2017b; Espenholt et al., 2018).

Value-based methods learn state-action values and select actions according to these values. One merit of value-based methods is to accurately control the exploration rate of the behavior policies by some trivial mechanism, such like ϵ -greedy. The drawback is also apparent. The policy improvement of valued-based methods totally depends on the policy evaluation. Unless the selected action is changed by a more accurate policy evaluation, the policy won't be improved. So the policy improvement of each policy iteration is limited, which leads to a low sample efficiency. Previous works equip valued-based methods with many appropriated designed structures, achieving a more promising sample efficiency (Wang et al., 2016; Schaul et al., 2015; Kapturowski et al., 2018).

Policy-based methods learn a parameterized policy directly without consulting state-action values. One merit of policy-based methods is that they incorporate a policy improvement phase every

training step, suggesting a more greedy use of samples to improve policy than value-based methods. Nevertheless, policy-based methods easily fall into a suboptimal solution, where the entropy drops to 0 (Haarnoja et al., 2018). The actor-critic methods introduce a value function as the baseline to reduce the variance of the policy gradient (Mnih et al., 2016), but maintain the other characteristics unchanged.

In this paper, we propose CASA-B, Critic **AS** an Actor with **B**andit **V**ote Algorithm, an innovative combination of the value-based and the policy-based methods, which adopts the merits and mitigates the drawbacks of both.

In general, CASA-B builds on the actor-critic design that estimates state values V , state-action values Q and policy π simultaneously. It integrates a consistent path between the policy evaluation and the policy improvement. It guarantees that **i**) the policy evaluation is equivalent to a compensational policy improvement for the function approximation error; **ii**) the policy evaluation regularizes the policy improvement, which means that CASA-B doesn't need any entropy regularization to prevent the policy from collapse.

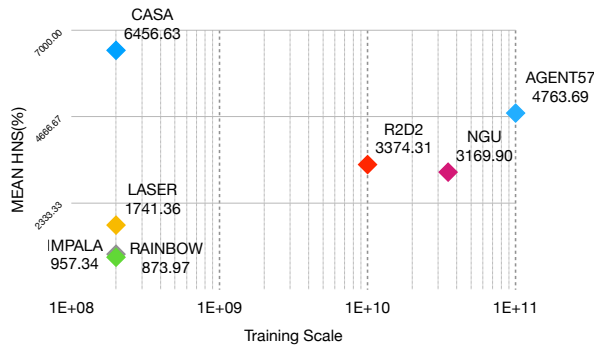


Figure 1: Mean Human Normalized Scores (%) of 57 games

CASA-B is capable of large scale training. Due to the fact that large scale training needs off-policy learning, we introduce Doubly-Robust Trace (DR-Trace), which **i**) exploits doubly-robust estimator to maximally reduce variances (Jiang, Li, 2016), **ii**) guarantees that Q and V converge synchronously to Q^* and V^* corresponding to the same policy.

To find a better exploration rate, we further introduce a progressive closed-form entropy control mechanism. As the deliberate design of CASA-B, the behavior policies that interact with the environment can achieve any desired entropy, which provides sufficient diversity for exploration.

We report our score on Arcade Learning Environment (ALE) (Bellemare et al., 2013; Machado et al., 2018). Our method achieves State-Of-The-Art (SOTA) among 200M scale algorithms and is also competitive compared with 10B+ scale algorithms.

Our main contributions are three fold:

- We propose an actor-critic design, which guarantees that
 - i**) the policy evaluation and the policy improvement share a consistent path,
 - ii**) the policy evaluation compensates function approximation error,
 - iii**) the policy evaluation regularizes the policy improvement from collapse.
- We propose DR-Trace and give a convergence proof.
- We propose an entropy control mechanism to adaptively adjust the exploration rate of the behavior policies.

2 BACKGROUND

Consider an infinite-horizon MDP, defined by $(\mathcal{S}, \mathcal{A}, p, r, \gamma)$, where \mathcal{S} is the state space, \mathcal{A} is the action space, $p : \mathcal{S} \times \mathcal{A} \times \mathcal{S} \rightarrow [0, 1]$ is the state transition probability function, $r : \mathcal{S} \times \mathcal{R} \rightarrow \mathbf{R}$ is the reward function, and γ is the discounted factor. Let $\pi : \mathcal{S} \times \mathcal{A} \rightarrow [0, 1]$ be the policy.

Define return $G_t = \sum_{k=0}^{\infty} \gamma^k r_{t+k}$, state value function $V^\pi(s_t) = \mathbf{E} [\sum_{k=0}^{\infty} \gamma^k r_{t+k} | s_t]$, state-action value function $Q^\pi(s_t, a_t) = \mathbf{E} [\sum_{k=0}^{\infty} \gamma^k r_{t+k} | s_t, a_t]$, and advantage function $A^\pi(s_t, a_t) =$

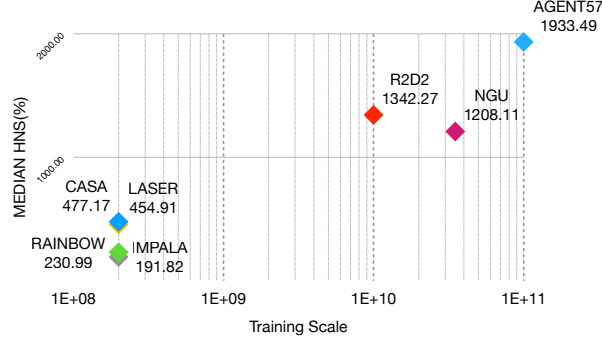


Figure 2: Median Human Normalized Scores (%) of 57 games

$Q^\pi(s_t, a_t) - V^\pi(s_t)$. The connections between V^π and Q^π is given by the Bellman equation,

$$\begin{aligned} \mathcal{T}Q^\pi(s_t, a_t) &= \mathbf{E}_p[r_t + \gamma V^\pi(s_{t+1})], \\ \text{where } V^\pi(s_t) &= \mathbf{E}_\pi[Q^\pi(s_t, a_t)]. \end{aligned}$$

The objective of reinforcement learning is to

$$\text{maximize } \mathcal{J} = \mathbf{E}_\pi \left[\sum_{k=0}^{\infty} \gamma^k r_k \right].$$

Value-based methods maximize \mathcal{J} by generalized policy iteration (GPI) (Sutton, Barto, 2018). The policy evaluation is conducted by minimizing $\mathbf{E}_\pi[(G - Q^\pi)^2]$, which gives the gradient ascent direction $\mathbf{E}_\pi[(G - Q^\pi)\nabla Q^\pi]$. The policy improvement is usually achieved by ϵ -greedy.

A refined structure design of Q^π is provided by (Wang et al., 2016). It estimates Q^π by the summation of the advantage function and the state value function, $Q^\pi = A^\pi + V^\pi$.

When large scale training is involved, the off-policy problem is inevitable. Denote μ as the behavior policy, π as the target policy. $c_t \stackrel{\text{def}}{=} \min\{\frac{\pi_t}{\mu_t}, \bar{c}\}$ is the clipped importance sampling. For brevity, $c_{[t:t+k]} \stackrel{\text{def}}{=} \prod_{i=0}^k c_{t+i}$. ReTrace (Munos et al., 2016) estimates $Q(s_t, a_t)$ by clipped per-step importance sampling

$$Q^{\tilde{\pi}}(s_t, a_t) = \mathbf{E}_\mu[Q(s_t, a_t) + \sum_{k \geq 0} \gamma^k c_{[t+1:t+k]} \delta_{t+k}^Q Q], \quad (1)$$

where $\delta_t^Q Q \stackrel{\text{def}}{=} r_t + \gamma Q(s_{t+1}, a_{t+1}) - Q(s_t, a_t)$. The above operator is a contraction mapping, and Q converges to $Q^{\tilde{\pi}_{\text{ReTrace}}}$ corresponding to some $\tilde{\pi}_{\text{ReTrace}}$.

Policy-based methods maximize \mathcal{J} by policy gradient. It's shown (Sutton, Barto, 2018) that $\nabla \mathcal{J} = \mathbf{E}_\pi[G \nabla \log \pi]$. When involved with a baseline, it becomes an actor-critic algorithm. The policy gradient is given by $\nabla \mathcal{J} = \mathbf{E}_\pi[(G - V^\pi) \nabla \log \pi]$, where V^π is optimized by minimizing $\mathbf{E}_\pi[(G - V^\pi)^2]$, giving the gradient ascent direction $\mathbf{E}_\pi[(G - V^\pi) \nabla V^\pi]$.

IMPALA (Espeholt et al., 2018) introduces V-Trace off-policy actor-critic algorithm to correct the discrepancy between the target policy and the behavior policy. Let $\rho_t \stackrel{\text{def}}{=} \min\{\frac{\pi_t}{\mu_t}, \bar{\rho}\}$. V-Trace estimates $V(s_t)$ by

$$V^{\tilde{\pi}}(s_t) = \mathbf{E}_\mu[V(s_t) + \sum_{k \geq 0} \gamma^k c_{[t:t+k-1]} \rho_{t+k} \delta_{t+k}^V V], \quad (2)$$

where $\delta_t^V V \stackrel{\text{def}}{=} r_t + \gamma V(s_{t+1}) - V(s_t)$. If $\bar{c} \leq \bar{\rho}$, the above operator is a contraction mapping, and V converges to $V^{\tilde{\pi}}$ that corresponds to

$$\tilde{\pi}(a|s) = \frac{\min\{\bar{\rho}\mu(a|s), \pi(a|s)\}}{\sum_{b \in \mathcal{A}} \min\{\bar{\rho}\mu(b|s), \pi(b|s)\}}.$$

The direction of the policy gradient is given by

$$\mathbf{E}_\mu [\rho_t(r_t + \gamma V^{\tilde{\pi}}(s_{t+1}) - V(s_t)) \nabla \log \pi].$$

Another related work is the maximum entropy framework (MaxEnt) (Haarnoja et al., 2017, 2018). The objective of MaxEnt is to

$$\text{maximize } \mathcal{J}_{soft} = \mathbf{E}_\pi \left[\sum_{k=0}^{\infty} \gamma^k (r_k + \tau \mathbf{H}[\pi]) \right].$$

Q_{soft}^π and V_{soft}^π are defined by the *soft* Bellman equation

$$\begin{aligned} \mathcal{T}Q_{soft}^\pi(s_t, a_t) &= \mathbf{E}_p[r_t + \gamma V_{soft}^\pi(s_{t+1})], \\ \text{where } V_{soft}^\pi(s_t) &= \mathbf{E}_\pi[Q_{soft}^\pi(s_t, a_t) - \tau \log \pi(a_t|s_t)]. \end{aligned} \quad (3)$$

π is defined as a Boltzmann policy

$$\pi \propto \exp((Q_{soft}^\pi(s_t, a_t) - V_{soft}^\pi(s_t))/\tau).$$

It's shown (Schulman et al., 2017a) that

$$\begin{aligned} \mathbf{E}_\pi[(q_t - Q_{soft}^\pi(s_t, a_t)) \nabla Q_{soft}^\pi(s_t, a_t)] \\ = \tau \nabla \mathcal{J}_{soft} + \mathbf{E}_\pi[(v_t - V_{soft}^\pi(s_t)) \nabla V_{soft}^\pi(s_t)].^1 \end{aligned} \quad (4)$$

The equation (4) demonstrates that *soft* Q-learning (SQL) is equivalent to the policy improvement of \mathcal{J}_{soft} and the policy evaluation of V_{soft}^π .

(Ghosh et al., 2020) regards the policy evaluation and the policy improvement as a projection operator and an improvement operator. It points out that an improvement operator compatible with the projection operator may be preferred. The consistency equation (4) fulfills such compatibility.

But there are some drawbacks: **i)** compared with the original \mathcal{J} , the objective \mathcal{J}_{soft} is regularized by the entropy, which means that Q_{soft}^π and V_{soft}^π are inconsistent with Q^π and V^π respectively, **ii)** although the temperature τ in \mathcal{J}_{soft} encourages the exploration by maximizing entropy reward when optimizing the target policy, it also couples the exploration rate of the behavior policy together with the target policy, which makes it difficult adjusting the exploration rate of the behavior policy freely for every episode.

3 CASA-B

3.1 Formulation

As stated above, current existing value-based methods, policy-based methods and their combinations are far from satisfactory. This motivates us to find the inherent connection between value-based methods and policy-based methods to integrate the merits of both.

Although MaxEnt suffers from some drawbacks, it's pretty close to unify value-based methods and policy-based methods. One observation is that \mathcal{J}_{soft} involves $\mathbf{H}[\pi]$ into \mathcal{J} , which bridges the policy evaluation and the policy improvement. When we restrict the objective back to \mathcal{J} , it's reasonable to conjecture that the policy evaluation and the policy improvement should be different, i.e.

$$\nabla \mathcal{J} \neq \text{constant} \cdot \mathbf{E}_\pi[(G - Q) \nabla Q],$$

where $\nabla \mathcal{J} = \mathbf{E}_\pi[(G - V) \nabla \log \pi]$. As $G - V$ and $G - Q$ represent the step size of the policy improvement direction $\nabla \log \pi$ and the policy evaluation direction ∇Q respectively, and $G - V \neq G - Q$, we won't expect the policy evaluation and the policy improvement to be equivalent, as long as we want to *maximize* \mathcal{J} . But inspired by the operator view (Ghosh et al., 2020), we conjecture a *weaker* consistent property that the policy improvement might be compatible with the policy evaluation:

Would there exist an appropriate structural design such that the policy improvement and the policy evaluation hold the path consistency, i.e. $\nabla Q \propto \nabla \log \pi$?

¹ $q_t = r_t + \gamma V_{soft}^\pi(s_{t+1})$. $v_t = V_{soft}^\pi(s_t) + \sum_{k=0}^{\infty} \gamma^k \delta_{t+k}$, where $\delta_t = r_t + \tau \mathbf{H}[\pi_t] + \gamma V_{soft}^\pi(s_{t+1}) - V_{soft}^\pi(s_t)$.

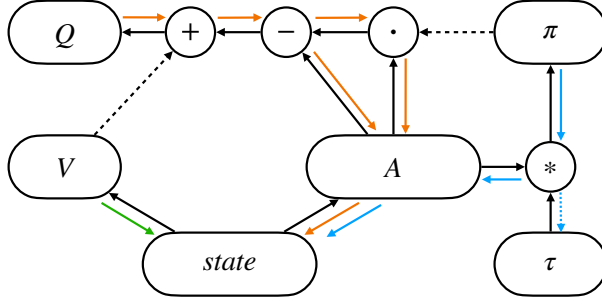


Figure 3: **Black** lines represent the forward process. **Dotted** black lines represent the *stop gradient* operator in the forward process. **Colorful** lines represent backpropagation from different loss functions. Specifically, **blue** lines represent $\mathbf{E}_\pi[(G - V)\nabla \log \pi]$, **orange** lines represent $\mathbf{E}_\pi[(G - Q)\nabla Q]$, and **green** lines represent $\mathbf{E}_\pi[(G - V)\nabla V]$.

Let's start from the Boltzmann policy, $\pi = \text{softmax}(A/\tau)$. Notice that π is a function of A . Now we want to find a function $Q = f(A, V)$ such that $\nabla Q \propto \nabla \log \pi$.

Lemma 1. *Let $g \in \mathcal{C}^1(\mathbf{R}^n) : \mathbf{R}^n \rightarrow \mathbf{R}^n$, $f \in \mathcal{C}^1(\mathbf{R}^{n+k}) : \mathbf{R}^{n+k} \rightarrow \mathbf{R}^n$. If $\nabla_x g(x) = \nabla_x f(x, y)$, for $\forall x \in \mathbf{R}^n, y \in \mathbf{R}^k$, then $\exists c \in \mathcal{C}^1(\mathbf{R}^k) : \mathbf{R}^k \rightarrow \mathbf{R}^n$, s.t. $f(x, y) = g(x) + c(y)$.*

Proof. See Appendix C, Lemma 1. □

Based on Lemma 1, we know $Q = f(A, V) = f_1(A) + f_2(V)$. According to the Bellman equation $\mathbf{E}_\pi[Q] = V$, we have

$$\mathbf{E}_\pi[f_1(A)] = \mathbf{E}_\pi[V - f_2(V)] = V - f_2(V).$$

Since $\mathbf{E}_\pi[f_1(A)]$ is not a function of V , taking $\partial/\partial V$ on both sides, we have that $V - f_2(V)$ is a constant function. Without loss of generality, we assume $V - f_2(V) = 0$, as we can minus this constant on both sides.

Now we know $Q = f(A) + V$.²

Since we won't change V when doing the policy improvement, we have $\partial \log \pi / \partial V = 0$. Noting that $\nabla Q \propto \nabla \log \pi \Rightarrow \partial Q / \partial V \propto \partial \log \pi / \partial V = 0$, we stop the gradient of V in $Q = f(A) + V$. Hence, we solve for f s.t. $\nabla f(A) \propto \nabla \log \pi$.

Lemma 2. *Define $\pi = \text{softmax}(A/\tau)$, then $\nabla \log \pi = (\mathbf{1} - \pi) \frac{\nabla A}{\tau}$. Denote sg to be stop gradient and define $\bar{A} = A - \mathbf{E}_\pi[A]$, $Q = \bar{A} + sg(V)$, then $\nabla Q = (\mathbf{1} - \pi) \nabla A$.*

Proof. See Appendix C, Lemma 2. □

By Lemma 2, we have

$$\nabla \log \pi = \frac{1}{\tau} (\mathbf{1} - \pi) \nabla A.$$

Notice that $\nabla \log \pi$ is the gradient ascent direction of the policy improvement, and $\nabla f(A)$ is the gradient ascent direction of the policy evaluation. If we regard π as a constant when evaluating π , we can integrate $(\mathbf{1} - \pi) \nabla A$ and get

$$f(A) \propto (\mathbf{1} - \pi)A + C.$$

Again, since $\mathbf{E}_\pi[Q] = V \Rightarrow \mathbf{E}_\pi[f(A)] = 0$, we know

$$Q = (\mathbf{1} - \pi)A + V = A - \mathbf{E}_\pi[A] + V.$$

Reformatting the above derivation, we have the forward process of CASA-B, shown in Figure 3.

²For simplicity, by abuse of notation, we write $Q = f_1(A) + V$ as $Q = f(A) + V$.

Denote $\tau \in \mathbf{R}_+$ to be a positive temperature, sg to be *stop gradient*. CASA-B estimates V , Q and π by

$$\begin{cases} A = A(s_t), & \pi = P(A/\tau), \\ V = V(s_t), & \bar{A} = A - E_\pi[A],^3 \quad Q = \bar{A} + sg(V). \end{cases} \quad (5)$$

Note that there exist two sg operators in (5). The first sg operator exists in $\bar{A} = A - E_\pi[A] = A - sg(\pi) \cdot A$. This sg operator guarantees the path consistency between the policy improvement and the policy evaluation, shown later in (12). Intuitively, this sg operator means that we keep π as a constant during the policy evaluation. The second sg operator exists in $Q = \bar{A} + sg(V)$. This sg operator is crucial in the convergence proof of Theorem 1. As (Chen, He, 2020) regards sg in siamese representation learning as a case of EM-algorithm (Dempster et al., 1977), a similar interpretation exists here. $Q = \bar{A} + sg(V)$ decomposes the estimation of Q into two parts, where the first is to estimate the advantage of each action without changing the expectation, the second is to estimate the expectation of Q .

Moreover, (5) is also a refinement of the structure of dueling- Q learning (Wang et al., 2016). We know dueling- Q estimates Q by $Q = A + V$, which is identical to the following Bellman equation

$$\mathcal{T}Q^\pi(s_t, a_t) = \mathbf{E}_p[r_t + \gamma V^\pi(s_{t+1}) - V^\pi(s_t)] + V^\pi(s_t).$$

Since $\mathbf{E}_\pi[\mathbf{E}_p[r_t + \gamma V^\pi(s_{t+1}) - V^\pi(s_t)]] = 0$, we have

$$\begin{aligned} \mathcal{T}Q^\pi(s_t, a_t) &= \mathbf{E}_p[(r_t + \gamma V^\pi(s_{t+1}) - V^\pi(s_t)) \\ &\quad - \mathbf{E}_\pi[\mathbf{E}_p[r_t + \gamma V^\pi(s_{t+1}) - V^\pi(s_t)]]] + V^\pi(s_t), \end{aligned}$$

which means $Q = A - E_\pi[A] + V$. In (5), we estimates Q exactly by $Q = \bar{A} + sg(V) = A - E_\pi[A] + sg(V)$. This formulation introduces the necessary condition $\mathbf{E}_\pi[Q] = V$, without loss of generality.

3.2 DR-Trace

In this section, we introduce how we learn (V, Q, π) .

One simple choice is to learn V and π by V-Trace (Espenholt et al., 2018) and to learn Q by ReTrace (Munos et al., 2016). (Espenholt et al., 2018) shows that, if $\bar{c} \leq \bar{\rho}$, $V^{\bar{\pi}}$ estimated by (2) converges to V^* that corresponds to some $\bar{\pi}_{VTrace}$. Respectively, (Munos et al., 2016) shows that $Q^{\bar{\pi}}$ estimated by (1) converges to Q^* that corresponds to some $\bar{\pi}_{ReTrace}$.

Though V-Trace learns (V, π) and ReTrace learns Q , it's inadequate. As CASA-B estimates (V, Q, π) , two questions come accordingly, **i**) how to guarantee that $\bar{\pi}_{VTrace} = \bar{\pi}_{ReTrace}$, **ii**) how to exploit (V, Q, π) to make a better estimation. Inspired by (Jiang, Li, 2016), which shows that the doubly robust estimator (DR) maximally reduces the variance, we introduce DR-Trace, which estimates V^π by

$$V_{DR}^{\bar{\pi}}(s_t) \stackrel{def}{=} \mathbf{E}_{\mu, p}[V(s_t) + \sum_{k \geq 0} \gamma^k c_{[t:t+k-1]} \rho_{t+k} \delta_{t+k}^{DR} V], \quad (6)$$

where $\delta_t^{DR} V \stackrel{def}{=} r_t + \gamma V(s_{t+1}) - Q(s_t, a_t)$.

With the one-step Bellman equation, we estimate Q^π by

$$\begin{aligned} Q_{DR}^{\bar{\pi}}(s_t, a_t) &\stackrel{def}{=} \mathbf{E}_{s_{t+1}, r_t \sim p(\cdot, \cdot | s_t, a_t)}[r_t + \gamma V_{DR}^{\bar{\pi}}(s_{t+1})] \\ &= \mathbf{E}_{\mu, p}[Q(s_t, a_t) + \sum_{k \geq 0} \gamma^k c_{[t+1:t+k-1]} \tilde{\rho}_{t,k} \delta_{t+k}^{DR} V], \end{aligned} \quad (7)$$

where $\tilde{\rho}_{t,k} = 1_{\{k=0\}} + 1_{\{k>0\}} \rho_{t+k}$.

³ $E_\pi[A] = sg(\pi) \cdot A$, where \cdot represents inner product.

Theorem 1. Define $\bar{A} = A - \mathbf{E}_\pi[A]$, $Q = \bar{A} + sg(V)$,

$$\mathcal{T}(Q) \stackrel{def}{=} \mathbf{E}_{\mu,p}[Q(s_t, a_t) + \sum_{k \geq 0} \gamma^k c_{[t+1:t+k-1]} \tilde{\rho}_{t,k} \delta_{t+k}^{DR} V],$$

$$\mathcal{S}(V) \stackrel{def}{=} \mathbf{E}_{\mu,p}[V(s_t) + \sum_{k \geq 0} \gamma^k c_{[t:t+k-1]} \rho_{t,k} \delta_{t+k}^{DR} V],$$

$$\mathcal{U}(Q, V) = (\mathcal{T}(Q) - \mathbf{E}_\pi[Q] + \mathcal{S}(V), \mathcal{S}(V)),$$

$$\mathcal{U}^{(n)}(Q, V) = \mathcal{U}(\mathcal{U}^{(n-1)}(Q, V)),$$

then $\mathcal{U}^{(n)}(Q, V) \rightarrow (Q^{\tilde{\pi}}, V^{\tilde{\pi}})$ that corresponds to

$$\tilde{\pi}(a|s) = \frac{\min\{\bar{\rho}\mu(a|s), \pi(a|s)\}}{\sum_{b \in \mathcal{A}} \min\{\bar{\rho}\mu(b|s), \pi(b|s)\}}.$$

as $n \rightarrow +\infty$.

Proof. See Appendix C, Theorem 1 □

Theorem 1 shows that operator ((6), (7)) is a contraction mapping and (V, Q) converges to (V^*, Q^*) that corresponds to

$$\tilde{\pi}(a|s) = \frac{\min\{\bar{\rho}\mu(a|s), \pi(a|s)\}}{\sum_{b \in \mathcal{A}} \min\{\bar{\rho}\mu(b|s), \pi(b|s)\}}. \quad (8)$$

At training time, the policy evaluation is achieved by updating θ to minimize $l2$ losses

$$\mathcal{V}(\theta) = \mathbf{E}_\pi[(V_\theta(s_t) - V_{DR}^{\tilde{\pi}}(s_t))^2]$$

concurrently with

$$\mathcal{Q}(\theta) = \mathbf{E}_\pi[(Q_\theta(s_t, a_t) - Q_{DR}^{\tilde{\pi}}(s_t, a_t))^2],$$

which gives the ascent direction of θ by

$$\begin{aligned} \nabla_\theta \mathcal{V}(\theta) &= \mathbf{E}_\pi [(V_{DR}^{\tilde{\pi}}(s_t) - V_\theta(s_t)) \nabla V_\theta(s_t)], \\ \nabla_\theta \mathcal{Q}(\theta) &= \mathbf{E}_\pi [(Q_{DR}^{\tilde{\pi}}(s_t, a_t) - Q_\theta(s_t, a_t)) \nabla Q_\theta(s_t, a_t)]. \end{aligned} \quad (9)$$

And we make the policy improvement by policy gradient, which gives the ascent direction of θ by

$$\nabla_\theta \mathcal{J}(\tau, \theta) = \mathbf{E}_\mu [\tau \rho_t (Q_{DR}^{\tilde{\pi}}(s_t, a_t) - V_\theta(s_t)) \nabla_\theta \log \pi_t], \quad (10)$$

where $\mathcal{J}(\tau, \theta) = \tau \mathbf{E}_\pi[\sum \gamma^t r_t]$. (10) takes an additional τ , which frees the scale of gradient from τ , shown in (12).

Finally, the gradient ascent direction of θ is given by

$$\xi \nabla_\theta \mathcal{V} + \alpha \nabla_\theta \mathcal{Q} + \beta \nabla_\theta \mathcal{J}. \quad (11)$$

Full algorithm is described in Appendix A. Note that (11) doesn't need any entropy regularization. We will discuss why this happens in section 3.3 and how CASA-B controls the exploration in section 3.5.

3.3 Path Consistency Between Policy Evaluation and Policy Improvement

From this section, we combine the coupled structure of π and Q in (5) and the gradient ascent direction (11) together, and discuss how the policy evaluation and the policy improvement affect each other.

With (V, Q, π) defined in (5), by Lemma 2, we have

$$\nabla_\theta Q = (\mathbf{1} - \pi) \nabla_\theta A = \tau \nabla_\theta \log \pi. \quad (12)$$

For brevity, denote $\mathbf{g} = (\mathbf{1} - \pi) \nabla_\theta A$.

Plugging (12) into (9) (10), we have

$$\nabla_{\theta} \mathcal{Q} = \mathbf{E}_{\pi} [(Q_t^{\bar{\pi}} - Q_t) \mathbf{g}], \nabla_{\theta} \mathcal{J} = \mathbf{E}_{\pi} [(Q_t^{\bar{\pi}} - V_t) \mathbf{g}].^4 \quad (13)$$

Recalling Theorem 1, when the importance sampling ratio $\bar{\rho} = +\infty$, we know $Q_t^{\bar{\pi}}$ is an unbiased estimation of $\mathbf{E}_{\pi}[G_t|s_t, a_t]$, ignoring the bias introduced by the function approximation error. Based on this observation, $\nabla_{\theta} \mathcal{Q}$ is a typical policy evaluation that Q converges to $\mathbf{E}_{\pi}[\sum \gamma^k r_k | s, a]$, and $\nabla_{\theta} \mathcal{J}$ is a typical policy improvement that maximizes $\mathbf{E}_{\pi}[\sum \gamma^k r_k]$. $\nabla_{\theta} \mathcal{Q}$ and $\nabla_{\theta} \mathcal{J}$ are expected to be different, as Q and V are updated by the Bellman equation, rather than the *soft* Bellman equation.

For equation (13), there is another thing in common, which is \mathbf{g} , the direction of the gradient. We call it a path. (13) shows that $\nabla_{\theta} \mathcal{Q}$ and $\nabla_{\theta} \mathcal{J}$ walk along the same path \mathbf{g} . The only difference is that $\nabla_{\theta} \mathcal{Q}$ walks with step size $Q_t^{\bar{\pi}} - Q_t$, but $\nabla_{\theta} \mathcal{J}$ walks with step size $Q_t^{\bar{\pi}} - V_t$. If we make a subtraction between $\nabla_{\theta} \mathcal{Q}$ and $\nabla_{\theta} \mathcal{J}$, we have

$$\nabla_{\theta} \mathcal{Q} = \nabla_{\theta} \mathcal{J} - \mathbf{E}_{\pi} [(Q_t - V_t) \mathbf{g}]. \quad (14)$$

We know $\mathbf{E}_{\pi} [(Q_t - V_t) \mathbf{g}]$ is also a policy gradient with function approximated Q_t . If we regard $Q_t^{\bar{\pi}}$ as a *better* estimation of Q_t , (14) says that the policy evaluation equals to the policy improvement minus a *worse* policy improvement, which is to retain the policy evaluation by pulling back from the policy improvement. As for how *worse* it is, it depends on how far Q_t is from $Q_t^{\bar{\pi}}$. Recalling (13) and $\mathbf{g} = \tau \nabla_{\theta} \log \pi$, we observe that if Q_t underestimates $Q_t^{\bar{\pi}}$, $\nabla_{\theta} \mathcal{Q}$ promotes $\pi(a_t|s_t)$ by $Q_t^{\bar{\pi}} - Q_t$, otherwise $\nabla_{\theta} \mathcal{Q}$ diminishes $\pi(a_t|s_t)$ by $Q_t^{\bar{\pi}} - Q_t$. So except for the policy evaluation, $\nabla_{\theta} \mathcal{Q}$ does do the policy improvement along the same path as $\nabla_{\theta} \mathcal{J}$, but only to compensate the estimation error of Q_t .

Based on (14), when we share all variables to estimate Q and π , except for τ , there is no gradient conflict. This is why we call the algorithm Critic AS an Actor. Compared with the methods that estimate π with another group of variables, CASA-B saves the quantity of variables for optimization.

Lemma 3. Define $\bar{A} = A - \mathbf{E}_{\pi}[A]$, $Q = \bar{A} + sg(V)$, $\pi = \text{softmax}(A/\tau)$, then $\mathbf{E}_{\pi} [(Q - V) \nabla \log \pi] = -\tau \nabla \mathbf{H}[\pi]$.

Proof. See Appendix C, Lemma 3. □

Now we know $\nabla_{\theta} \mathcal{Q}$ is not only a policy evaluation but is also equivalent to a compensational policy improvement. If we further exploit the structural information, by Lemma 3,

$$\mathbf{E}_{\pi} [(Q_t - V_t) \mathbf{g}] = \tau \mathbf{E}_{\pi} [(Q_t - V_t) \nabla_{\theta} \log \pi] = -\tau^2 \nabla_{\theta} \mathbf{H}[\pi],$$

we have

$$\nabla_{\theta} \mathcal{Q} = \nabla_{\theta} \mathcal{J} + \tau^2 \nabla_{\theta} \mathbf{H}[\pi]. \quad (15)$$

(15) shows another explanation of $\nabla_{\theta} \mathcal{Q}$, which is a policy gradient with entropy regularization. As long as $\alpha > 0$ in (11), an entropy regularization is introduced by $\alpha \nabla_{\theta} \mathcal{Q}$. An intuitive explanation is that, as Q and π share A , but the target of Q is dominated by MDP, so Q regularizes A to prevent π from collapse to trivial solutions.

3.4 Comparison to MaxEnt

As CASA-B defines a Boltzmann policy, and (15) is similar to MaxEnt (Haarnoja et al., 2017, 2018), in this section, we'll discuss connections between CASA-B and MaxEnt.

Recalling (4), since $\mathcal{J}_{soft} = \mathcal{J}/\tau + \tau \mathbf{H}$, we have

$$\begin{aligned} \nabla_{\theta} \mathcal{Q}_{soft} &= \tau \nabla_{\theta} \mathcal{J}_{soft} + \nabla_{\theta} \mathcal{V}_{soft} \\ &= \nabla_{\theta} \mathcal{J} + \tau^2 \nabla_{\theta} \mathbf{H}[\pi] + \nabla_{\theta} \mathcal{V}_{soft}. \end{aligned}$$

(15) doesn't contain $\nabla_{\theta} \mathcal{V}_{soft}$, compared with the above equation. Recalling (3), \mathcal{V}_{soft} is precisely the term that involves *soft*, which makes the *soft* Bellman equation different from the Bellman equation.

⁴ $Q_t^{\bar{\pi}} = Q_{DR}^{\bar{\pi}}(s_t, a_t)$, $Q_t = Q(s_t, a_t)$, $V_t = V(s_t)$.

For MaxEnt, since $\pi \propto \exp(Q_{soft}/\tau)$, we have

$$Q_{soft} = \tau \log \pi + \tau \log \int_{\mathcal{A}} \exp(Q_{soft}/\tau).$$

With the definition of $V_{soft} = \tau \log \int_{\mathcal{A}} \exp(Q_{soft}/\tau)$, it's shown that $\nabla Q = \tau \nabla \log \pi + \nabla V_{soft}$, where V_{soft} is retained and has to be estimated.

For CASA-B, since $\pi \propto \exp(A/\tau)$, we have

$$\begin{aligned} A &= \tau \log \pi + \tau \log \int_{\mathcal{A}} \exp(A/\tau) \\ &= \tau \log \pi + \tau \log \int_{\mathcal{A}} \exp(Q/\tau) - V \\ &= \tau \log \pi + V_{soft} - V. \end{aligned}$$

So we have

$$Q = A - \mathbf{E}_{\pi}[A] + V = \tau \log \pi - \tau \mathbf{E}_{\pi}[\log \pi] + V,$$

which eliminates V_{soft} by $A - \mathbf{E}_{\pi}[A]$ and adds an independently estimated V . This is how CASA-B removes *soft*.

Note that the objective of CASA-B is \mathcal{J} , which won't change the original MDP. For CASA-B, adjusting τ arbitrarily won't change the transition probability distribution of the original MDP. But for MatEnt, as the objective is \mathcal{J}_{soft} , the entropy of the behavior policies' and the target policy's can't be disentangled. Adjusting τ in \mathcal{J}_{soft} will result in the change of the transition probability distribution, specifically, the reward function. Namely, making entropy control of MaxEnt will result in an unstable policy evaluation.

3.5 Adaptive Entropy Control

In this section, we introduce how CASA-B controls the exploration rate of the behavior policies. Denote the class of Boltzmann policies defined in (5) as

$$\pi(\tau) \propto \exp(A/\tau).$$

It's evident that, $\mathbf{H}[\pi(\tau)] \rightarrow 0$, $\pi(\tau) \rightarrow \text{argmax}$, as $\tau \rightarrow 0+$; $\mathbf{H}[\pi(\tau)] \rightarrow \log |\mathcal{A}|$, $\pi(\tau) \rightarrow \text{uniform}$, as $\tau \rightarrow +\infty$. Since $\mathbf{H}[\pi(\tau)]$ is a continuous function w.r.t. τ , for any desired entropy e , we can always find a τ_0 s.t. $\mathbf{H}[\pi(\tau_0)] = e$. So we can simply control $\mathbf{H}[\pi(\tau)]$ by choosing a proper τ .

As (V, Q) satisfies the following Bellman equation,

$$\begin{aligned} \mathcal{T}Q_t &= \mathbf{E}_p[r_t + \gamma V_{t+1}], \\ \text{where } V_t &= \mathbf{E}_{\pi(\tau)}[Q_t], \end{aligned}$$

we observe that τ only influences (V, Q) when taking the expectation $V_t = \mathbf{E}_{\pi(\tau)}[Q_t]$. If τ is sampled from some distribution Ω , the influence is totally eliminated as

$$\begin{aligned} \mathcal{T}Q_t &= \mathbf{E}_p[r_t + \gamma V_{t+1}], \\ \text{where } V_t &= \mathbf{E}_{\tau \sim \Omega}[\mathbf{E}_{\pi(\tau)}[Q_t]], \end{aligned}$$

Now Q_t only depends on the MDP's transition probability and the *average* policy $\pi(\Omega) \stackrel{\text{def}}{=} \int_{\tau \sim \Omega} \pi(\tau)$.

Lemma 4. *Let $v \in \mathbf{R}^{|\mathcal{A}|}$ to be a vector. Define $\pi(\tau) = \exp(v/\tau)/Z$, $Z = \int_{\mathcal{A}} \exp(v/\tau)$. Let Ω to be a probability measure supported on $[K, +\infty]$, then $f(\Omega) = \mathbf{E}_{\tau \sim \Omega}[\mathbf{E}_{\pi(\tau)}[v]]$ satisfies Lipschitz-1 condition with Wasserstein-1 metric.*

Proof. See Appendix C, Lemma 4. □

Lemma 4 shows, if Ω is supported on a finite closed interval $[K, +\infty]$, the change of $\mathbf{E}_{\tau \sim \Omega}[\mathbf{E}_{\pi(\tau)}[Q_t]]$ can be bounded by the change of Ω . Hence, we can progressively change Ω such that $\mathbf{H}[\pi(\Omega)]$ locates in the desired region, without introducing much variance into the policy evaluation.

In practice, we use a Bandits Vote Algorithm (BVA) to improve Ω , which adaptively controls the exploration rate of $\pi(\Omega)$. **The details are described in Appendix B.**

4 Experiments

In this section, we firstly introduce our basic setup. Then we report our results on ALE, specifically, 57 atari games. To further investigate how CASA-B works, we study the effects of *sg* operators, DR-Trace, BVA, and path consistency.

4.1 Basic Setup

	HNS(%)		SABER(%)	
	Mean	Median	Mean	Median
CASA-B	6456.63	477.17	50.11	13.90
Rainbow	873.97	230.99	28.39	4.92
IMPALA	957.34	191.82	29.45	4.31
LASER	1741.36	454.91	36.77	8.08
R2D2	3374.31	1342.27	60.43	33.62
NGU	3169.90	1208.11	50.47	21.19
Agent57	4763.69	1933.49	76.26	43.62

Table 1: Atari Scores. Rainbow’s scores are from (Hessel et al., 2017). IMPALA’s scores are from (Espeholt et al., 2018). LASER’s scores are from (Schmitt et al., 2020), no sweep at 200M. R2D2’s scores are from (Kapturowski et al., 2018). NGU’s scores are from (Badia et al., 2020b). Agent57’s scores are from (Badia et al., 2020a).

We use Learner-Actor architecture for large scale training. To deal with partially observable MDP (POMDP), we use a recurrent encoder by LSTM (Schmidhuber, 1997) with 256 units. We use *burn-in* (Kapturowski et al., 2018) to deal with representational drift. We store the recurrent state during inference and make it the start point of the *burn-in* phase. We train each sample twice.

We don’t use any intrinsic reward in any experiment. To be general, we won’t end the episode if life is lost. The reward is reshaped by $\log(\text{abs}(r) + 1.0) \cdot (2 \cdot 1_{\{r \geq 0\}} - 1_{\{r < 0\}})$. No reward clipping is applied.

To stabilize training, we use two auxiliary tasks. The first is the forward dynamic prediction, which learns $s_t, a_t \rightarrow s_{t+1}$. Different from the pixel control method (Jaderberg et al., 2016), the task is performed in the latent space. The second is the inverse dynamic prediction, which learns $s_t, s_{t+1} \rightarrow a_t$. We use the contingency-aware action prediction (Choi et al., 2018). Note that we only perform the inverse dynamic task regardless later parts for computing the intrinsic reward.

We use BVA to sample τ s, evaluate τ s and find the best region of τ s. We use τ s sampled from this best region to approximate the expected return. **Hyperparameters are listed in Appendix D.**

4.2 Analysis and Summary of Results

Table 1 summarizes the mean and the median Human Normalized Scores (HNS)⁵ of 57 games. **Scores of 57 games and the corresponding learning curves are listed in Appendix F.** The videos will be released in the future.

In general, CASA-B is trained with 200M samples without any intrinsic reward and achieves SOTA on mean HNS compared with other algorithms, including 10B+ algorithms (R2D2, NGU, AGENT57). Although there is room for improvement on median HNS compared with 10B+ algorithm with larger training scale, it should be mentioned that it is far more sample efficient to achieve this SOTA result.

The results can roughly be classified into three kinds:

- i) results of some games achieve *FS*, such as Atlantis, Gopher, Jamesbond;
- ii) results of some games are increasing and the learning processes haven’t converged, such as Alien, BeamRider, ChopperCommand;

⁵ $HNS = \frac{G - G_{random}}{G_{Human} - G_{random}}$.

iii) results of some games encounter the bottleneck due to the hard exploration problem, such as IceHockey, PrivateEye, Surround.

ii) suggests two potential directions for improvement. One is that CASA-B can achieve higher scores on these games with larger training scale. The other is that there is room for higher sample efficiency, compared with LASER on Alien, Centipede, etc.

One crucial thing for solving **iii)** is how samples are produced, which will be discussed in our ablation study. CASA-B tries to collect diverse samples by enlarging the behavior policy to a family of policies $\{\pi(\tau)\}_{\tau \in [K, +\infty]}$. The family can achieve any desired entropy. However, it’s obvious that $\pi(\tau)$ is an order-preserving mapping of A , which means that the total order relations of actions’ probability distributions are identical for $\forall \pi(\tau) \in \{\pi(\tau)\}_{\tau \in [K, +\infty]}$. Value-based methods such as R2D2 collect samples by a family of policies $\{\pi_\epsilon\}_{\epsilon \in [0, 1]}$, where π_ϵ represents ϵ -greedy. Except for the max Q -value, π_ϵ doesn’t preserve the order. $\{\pi_\epsilon\}_{\epsilon \in [0, 1]}$ is more likely to explore the state where $\{\pi(\tau)\}_{\tau \in [K, +\infty]}$ less prefers, but the efficiency is low as such exploration mainly depends on *luck*. Instead, NGU and Agent57 achieve active exploration of the environment by the intrinsic reward. Such exploration enlarges the original MDP, so UVFA is involved to deal with the impact of the shift.

CASA-B focuses on the original MDP. There are some hints to improve CASA-B. The first is to relax the path consistency by a linear combination. Since π_ϵ is identical to $\epsilon \cdot \pi(+\infty) + (1 - \epsilon) \cdot \pi(0+)$, it’s reasonable to consider a combination representation for a larger family of behavior policies. The second is to adopt the idea of LASER by shared experience replay, which gives diverse samples from different families of policies $\{\{\pi_n(\tau)\}_{\tau \in [K, +\infty]}\}_{n=1, 2, \dots}$. The third is to make a better policy evaluation. Now the value estimation is w.r.t. the *average* policy $\pi(\Omega)$, which is $V_{\pi(\Omega)}$. A better way is to use a UVFA or a closed-form expression, if exists, to estimate $\{V_{\pi(\tau)}\}_{\tau \in [K, +\infty]}$.

4.3 Ablation Study

In our ablation study, we consider the effects of the following techniques and properties of CASA-B,

- i)** *stop gradient* of π in $\bar{A} = A - \mathbf{E}_\pi[A] = A - sg(\pi) \cdot A$ in (5), which gives the path consistency;
- ii)** *stop gradient* of V in $Q = \bar{A} + sg(V)$ in (5), which is essential in the convergence proof of Theorem 1;
- iii)** DR-Trace, which is to reduce the variance of the policy evaluation maximally;
- iv)** path consistency between the policy evaluation and the policy improvement;
- v)** enlarged policy family $\{\pi(\tau)\}_{\tau \in [K, +\infty]}$, which allows the behavior policy to achieve any desired entropy;
- vi)** BVA, which adaptive searches for Ω .

Our ablation experiments are designed as follows.

- To verify **i)** and **ii)**, we simply remove the corresponding *stop gradient* in our actor-critic design, named as *no_stop_pi* and *no_stop_v* respectively.
- To verify **iii)**, we use V-Trace to estimate *vs* and ReTrace to estimate *qs*, named as *no_drtrace*.
- To verify **iv)**, we randomly sample Q -loss scaling α and π -loss scaling β from *Uniform*([0, 20]) for every sample of every batch, named as *random_scaling*.
- To verify **v)**, we train a single trainable τ instead of sampling τ from BVA, named as *trainable_tau*.
- To verify **vi)**, we sample τ from the fixed initial distribution without updating BVA, named as *no_bva*.

More details of the ablation experiments are described in Appendix E.

no_stop_pi and *no_stop_v* perform much worse than CASA-B, which empirically confirms that *stop gradient* operators are necessary for (5).

There is no evident difference between *no_drtrace* and CASA-B, as *no_drtrace* is better than CASA-B on Hero and Qbert, but worse on others. But the variance of *no_drtrace* is higher, which coincides with the fact that DR maximally reduce the variance.

Except for Qbert, *random_scaling* performs similar to CASA-B, which empirically shows that CASA-B is robust to Q -loss scaling and π -loss scaling as their paths are consistent.

It’s interesting to compare CASA-B, *trainable_tau*, and *no_bva*. Intuitively, *trainable_tau* is the most greedy one that collects samples from the latest trained single policy, and *no_bva* is the most diverse

one that collects samples from a family of policies with a fixed distribution of temperature. This is reflected by the entropy of the policies in Figure 5, where *trainable_tau* has the smallest entropy and *no_bva* has the largest entropy. However, there doesn't exist a comprehensive advantage schema to collect samples. *no_bva* performs worse than CASA-B in general. *trainable_tau* reaches FS on ChopperCommand i.e. 999k, but *trainable_tau* is less stable than CASA-B and much worse on Qbert.

Such phenomenon has been claimed by DisCor (Kumar et al., 2020): *the choice of the sampling distribution is of crucial importance for the stability and efficiency of ADP algorithms*. With a given replay buffer, DisCor reweights each sample to mitigate this phenomenon. But if working on sample acquiring rather than sample re-weighting, it's an interesting question to find a proper family of behavior policies such that the policy learned with collected samples on the specific MDP can achieve higher sample efficiency. We leave this question for future study.

5 Conclusion

This paper proposes an innovative actor-critic design, which bridges the policy evaluation and the policy improvement by a consistent path. Based on it, we propose DR-Trace and prove the convergence. Also, we propose an adaptive entropy control mechanism and prove the Lipschitz condition, instantiated as the Bandit Vote Algorithm in practice.

Our method is sample efficient and achieves new SOTA among 200M scale algorithms. Our method is also very competitive compared with 10B+ scale algorithms. We analyse the ablation cases and discuss the potential improvement of the method in future work.

References

- Badia Adrià Puigdomènech, Piot Bilal, Kapturowski Steven, Sprechmann Pablo, Vitvitskyi Alex, Guo Daniel, Blundell Charles. Agent57: Outperforming the atari human benchmark // arXiv preprint arXiv:2003.13350. 2020a.
- Badia Adrià Puigdomènech, Sprechmann Pablo, Vitvitskyi Alex, Guo Daniel, Piot Bilal, Kapturowski Steven, Tieleman Olivier, Arjovsky Martín, Pritzel Alexander, Bolt Andrew, others . Never Give Up: Learning Directed Exploration Strategies // arXiv preprint arXiv:2002.06038. 2020b.
- Bellemare M. G., Naddaf Y., Veness J., Bowling M. The Arcade Learning Environment: An Evaluation Platform for General Agents // Journal of Artificial Intelligence Research. jun 2013. 47. 253–279.
- Chen Xinlei, He Kaiming. Exploring Simple Siamese Representation Learning // arXiv preprint arXiv:2011.10566. 2020.
- Choi Jongwook, Guo Yijie, Moczudilski Marcin, Oh Junhyuk, Wu Neal, Norouzi Mohammad, Lee Honglak. Contingency-aware exploration in reinforcement learning // arXiv preprint arXiv:1811.01483. 2018.
- Dempster A. P., Laird N. M., Rubin D. B. Maximum likelihood from incomplete data via the EM algorithm // JOURNAL OF THE ROYAL STATISTICAL SOCIETY, SERIES B. 1977. 39, 1. 1–38.
- Epesholt Lasse, Soyer Hubert, Munos Remi, Simonyan Karen, Mnih Volodymir, Ward Tom, Doron Yotam, Firoiu Vlad, Harley Tim, Dunning Iain, others . Impala: Scalable distributed deep-rl with importance weighted actor-learner architectures // arXiv preprint arXiv:1802.01561. 2018.
- Ghosh Dibya, Machado Marlos C., Roux Nicolas Le. An operator view of policy gradient methods // ArXiv. 2020. abs/2006.11266.
- Haarnoja Tuomas, Tang Haoran, Abbeel Pieter, Levine Sergey. Reinforcement learning with deep energy-based policies // arXiv preprint arXiv:1702.08165. 2017.
- Haarnoja Tuomas, Zhou Aurick, Abbeel Pieter, Levine Sergey. Soft actor-critic: Off-policy maximum entropy deep reinforcement learning with a stochastic actor // arXiv preprint arXiv:1801.01290. 2018.

- Hessel Matteo, Modayil Joseph, Van Hasselt Hado, Schaul Tom, Ostrovski Georg, Dabney Will, Horgan Dan, Piot Bilal, Azar Mohammad, Silver David.* Rainbow: Combining improvements in deep reinforcement learning // arXiv preprint arXiv:1710.02298. 2017.
- Jaderberg Max, Mnih Volodymyr, Czarnecki Wojciech Marian, Schaul Tom, Leibo Joel Z, Silver David, Kavukcuoglu Koray.* Reinforcement learning with unsupervised auxiliary tasks // arXiv preprint arXiv:1611.05397. 2016.
- Jiang Nan, Li Lihong.* Doubly robust off-policy value evaluation for reinforcement learning // International Conference on Machine Learning. 2016. 652–661.
- Kapturovski Steven, Ostrovski Georg, Quan John, Munos Remi, Dabney Will.* Recurrent experience replay in distributed reinforcement learning // International conference on learning representations. 2018.
- Kumar Aviral, Gupta Abhishek, Levine Sergey.* Discor: Corrective feedback in reinforcement learning via distribution correction // arXiv preprint arXiv:2003.07305. 2020.
- Machado Marlos C., Bellemare Marc G., Talvitie Erik, Veness Joel, Hausknecht Matthew J., Bowling Michael.* Revisiting the Arcade Learning Environment: Evaluation Protocols and Open Problems for General Agents // Journal of Artificial Intelligence Research. 2018. 61. 523–562.
- Mnih Volodymyr, Badia Adrià Puigdomènech, Mirza Mehdi, Graves Alex, Lillicrap Timothy P, Harley Tim, Silver David, Kavukcuoglu Koray.* Asynchronous Methods for Deep Reinforcement Learning. 2016.
- Mnih Volodymyr, Kavukcuoglu Koray, Silver David, Rusu Andrei A, Veness Joel, Bellemare Marc G, Graves Alex, Riedmiller Martin, Fidjeland Andreas K, Ostrovski Georg, others .* Human-level control through deep reinforcement learning // nature. 2015. 518, 7540. 529–533.
- Munos Remi, Stepleton Tom, Harutyunyan Anna, Bellemare Marc.* Safe and Efficient Off-Policy Reinforcement Learning // Advances in Neural Information Processing Systems 29. 2016. 1054–1062.
- Pedersen Carsten Lund.* RE: Human-level Performance in 3D Multiplayer Games with Population-based Reinforcement Learning // Science. 2019.
- Schaul Tom, Quan John, Antonoglou Ioannis, Silver David.* Prioritized experience replay // arXiv preprint arXiv:1511.05952. 2015.
- Schmidhuber Sepp Hochreiter; Jürgen.* Long short-term memory // Neural Computation. 1997.
- Schmitt Simon, Hessel Matteo, Simonyan Karen.* Off-policy actor-critic with shared experience replay // International Conference on Machine Learning. 2020. 8545–8554.
- Schulman John, Chen Xi, Abbeel Pieter.* Equivalence between policy gradients and soft q-learning // arXiv preprint arXiv:1704.06440. 2017a.
- Schulman John, Levine Sergey, Abbeel Pieter, Jordan Michael, Moritz Philipp.* Trust region policy optimization // International conference on machine learning. 2015. 1889–1897.
- Schulman John, Wolski Filip, Dhariwal Prafulla, Radford Alec, Klimov Oleg.* Proximal policy optimization algorithms // arXiv preprint arXiv:1707.06347. 2017b.
- Sutton Richard S, Barto Andrew G.* Reinforcement learning: An introduction. 2018.
- Vinyals Oriol, Babuschkin Igor, Czarnecki Wojciech M, Mathieu Michaël, Dudzik Andrew, Chung Junyoung, Choi David H, Powell Richard, Ewalds Timo, Georgiev Petko, others .* Grandmaster level in StarCraft II using multi-agent reinforcement learning // Nature. 2019. 575, 7782. 350–354.
- Wang Ziyu, Schaul Tom, Hessel Matteo, Hasselt Hado, Lanctot Marc, Freitas Nando.* Dueling network architectures for deep reinforcement learning // International conference on machine learning. 2016. 1995–2003.

A CASA-B Algorithm

Our training algorithm is shown in **Algorithm 1**, where we describe how learners and actors work asynchronously.

Algorithm 1 CASA-B Algorithm.

```

Initialize Parameter Server (PS) and Data Collector (DC).

// LEARNER
Initialize  $d_{push}$ .
Initialize  $\theta$ , i.e. initialize  $A_\theta, V_\theta$ , and calculate  $Q_\theta$  and  $\pi_\theta$  as in (5).
Initialize  $count = 0$ .
while True do
  Load data from DC.
  Estimate  $vs$  by (6) and estimate  $qs$  by (7).
  Update  $\theta$  by (11).
  if  $count \bmod d_{push} = 0$  then
    Push  $\theta$  to PS.
  end if
   $count \leftarrow count + 1$ .
end while

// ACTOR
Initialize  $d_{pull}, M$ .
Initialize  $\theta$ , i.e. initialize  $A_\theta, V_\theta$ , and calculate  $Q_\theta$  and  $\pi_\theta$  as in (5).
Initialize  $\{\mathcal{B}_m\}_{m=1,\dots,M}$  and sample  $\tau$  as in Algorithm 2.
Initialize  $count = 0, G = 0$ .
while True do
  Calculate  $\pi(\tau)(\cdot|s)$ .
  Sample  $a \sim \pi(\tau)(\cdot|s)$ .
   $s, r, done \sim p(\cdot|s, a)$ .
   $G \leftarrow G + r$ .
  if done then
    Update  $\{\mathcal{B}_m\}_{m=1,\dots,M}$  with  $(\tau, G)$  as in Algorithm 2.
    Send data to DC and reset the environment.6
     $G \leftarrow 0$ .
    Sample  $\tau$  as in Algorithm 2
  end if
  if  $count \bmod d_{pull} = 0$  then
    Pull  $\theta$  from PS and update  $\theta$ .
  end if
   $count \leftarrow count + 1$ .
end while

```

⁶In practice, to save memory usage, we pre-send data back as long as the trajectory length surpasses recurrent sequence length.

B Bandits Vote Algorithm

In practice, we use a Bandits Vote Algorithm (BVA) to adaptively control the entropy of the *average* policy $\mathbf{H}[\pi(\Omega)]$.

The algorithm is shown in **Algorithm 2**.

Algorithm 2 Bandits Vote Algorithm.

```

for  $m = 1, \dots, M$  do
  Sample  $mode \sim \{argmax, random\}$ , sample  $lr$ , sample  $width$ .
  Initialize  $B_m = Bandit(mode, l, r, acc, width, lr, \mathbf{w}, \mathbf{N}, d)$ .
end for
while  $True$  do
  for  $m = 1, \dots, M$  do
    Evaluate  $\mathcal{B}_m$  by (16).
    Sample candidates  $c_{m,1}, \dots, c_{m,d}$  by  $mode$  and (18) from  $\mathcal{B}_m$ .
  end for
  Sample  $x$  from  $\{c_{m,i}\}_{m=1, \dots, M; i=1, \dots, d}$ .
  Execute  $x$  and receive  $g$ .
  for  $m = 1, \dots, M$  do
    Update  $\mathcal{B}_m$  with  $(x, g)$  by (17).
  end for
end while

```

Let's firstly define a bandit as $\mathcal{B} = Bandit(mode, l, r, acc, width, lr, \mathbf{w}, \mathbf{N}, d)$.

- $mode$ is the mode of sampling, with two choices, $argmax$ and $random$.
- l is the left boundary of \mathcal{B} , and each x is clipped to $x = \max\{x, l\}$.
- r is the right boundary of \mathcal{B} , and each x is clipped to $x = \min\{x, r\}$.
- acc is the accuracy, where each x is located in the $\lfloor (\min\{\max\{x, l\}, r\} - l) / acc \rfloor$ th tile.
- $width$ is the tile coding width, where the value of the i th tile is estimated by the average of $\{\mathbf{w}_{i-width}, \dots, \mathbf{w}_{i+width}\}$.
- lr is the learning rate.
- \mathbf{w} is a vector in $\mathbf{R}^{\lfloor (r-l)/acc \rfloor}$, which represents the weight of each tile.
- \mathbf{N} is a vector in $\mathbf{R}^{\lfloor (r-l)/acc \rfloor}$, which counts the number of sampling of each tile.
- d is an integer, which represents how many candidates is provided by \mathcal{B} when sampling.

During the evaluation process, we evaluate the value of the i th tile by

$$V_i = \frac{1}{2 * width + 1} \sum_{k=i-width}^{i+width} \mathbf{w}_k. \quad (16)$$

During the training process, for each sample (x, g) , where g is the target value. Since x locates in the i th tile, we update \mathcal{B} by

$$\begin{cases} i = \lfloor (\min\{\max\{x, l\}, r\} - l) / acc \rfloor, \\ \mathbf{w}_j \leftarrow \mathbf{w}_j + lr * (g - V_i), j = i - width, \dots, i + width, \\ \mathbf{N}_i \leftarrow \mathbf{N}_i + 1. \end{cases} \quad (17)$$

During the sampling process, we firstly evaluate \mathcal{B} by (16) and get $(V_1, \dots, V_{\lfloor (r-l)/acc \rfloor})$. We calculate the score of i th tile by

$$score_i = \frac{V_i - \mu(\{V_j\}_{j=1, \dots, \lfloor (r-l)/acc \rfloor})}{\sigma(\{V_j\}_{j=1, \dots, \lfloor (r-l)/acc \rfloor})} + c \cdot \sqrt{\frac{\log(1 + \sum_j \mathbf{N}_j)}{1 + \mathbf{N}_i}}. \quad (18)$$

⁷For the boundary case, we change the summation indexes and the denominator accordingly.

For different *modes*, we sample the candidates by the following mechanism,

- if *mode* = *argmax*, find tiles with top-*d* scores, then sample *d* candidates from these tiles, one uniformly from a tile;
- if *mode* = *random*, sample *d* tiles with scores as the logits without replacement, then sample *d* candidates from these tiles, one uniformly from a tile;

In practice, we define a set of bandits $\{B_m\}_{m=1,\dots,M}$. At each step, we sample *d* candidates $\{c_{m,i}\}_{i=1,\dots,d}$ from each B_m , so we have a set of $m \times d$ candidates $\{c_{m,i}\}_{m=1,\dots,M;i=1,\dots,d}$. Then we sample uniformly from these $m \times d$ candidates to get x . At last, we transform the selected x to τ by $\tau = \frac{1}{\exp(x)-1}$. When we receive (τ, g) , we transform τ to x by $x = \log(1 + 1/\tau)$. Then we update each B_m by (17).

C Proofs

Lemma 1. Let $g \in C^1(\mathbf{R}^n) : \mathbf{R}^n \rightarrow \mathbf{R}^n$, $f \in C^1(\mathbf{R}^{n+k}) : \mathbf{R}^{n+k} \rightarrow \mathbf{R}^n$. If $\nabla_x g(x) = \nabla_x f(x, y)$, for $\forall x \in \mathbf{R}^n, y \in \mathbf{R}^k$, then $\exists c \in C^1(\mathbf{R}^k) : \mathbf{R}^k \rightarrow \mathbf{R}^n$, s.t. $f(x, y) = g(x) + c(y)$.

Proof. Let $\tilde{f}(x, y) = f(x, y) - g(x)$.

Since $\nabla_x g(x) = \nabla_x f(x, y)$, we have

$$\nabla_x \tilde{f} = 0, \text{ for } \forall x \in \mathbf{R}^n, y \in \mathbf{R}^k.$$

So \tilde{f} is a constant function w.r.t x , which can be denoted as $c(y) = \tilde{f}(x, y)$.

Hence, $f(x, y) = g(x) + c(y)$. \square

Lemma 2. Define $\pi = \text{softmax}(A/\tau)$, then $\nabla \log \pi = (\mathbf{I} - \pi) \frac{\nabla A}{\tau}$. Denote sg to be stop gradient and define $\bar{A} = A - \mathbf{E}_\pi[A]$, $Q = \bar{A} + sg(V)$, then $\nabla Q = (\mathbf{I} - \pi) \nabla A$.

Proof. As $Q = \bar{A} + sg(V) = A - sg(\pi) \cdot A + sg(V)$, it's obvious that $\nabla Q = (\mathbf{I} - \pi) \nabla A$.

For $\log \pi$, it's a typical derivative of cross entropy, so we have $\nabla \log \pi = (\mathbf{I} - \pi) \nabla(A/\tau) = (\mathbf{I} - \pi) \frac{\nabla A}{\tau}$. \square

Lemma 3. Define $\bar{A} = A - \mathbf{E}_\pi[A]$, $Q = \bar{A} + sg(V)$, $\pi = \text{softmax}(A/\tau)$, then

$$\mathbf{E}_\pi [(Q - V) \nabla \log \pi] = -\tau \nabla \mathbf{H}[\pi].$$

Proof. Since

$$\pi = \exp(A/\tau)/Z, \quad Z = \int_{\mathcal{A}} \exp(A/\tau),$$

we have

$$A = \tau \log \pi + \tau \log Z.$$

Based on the observation that $\mathbf{E}_\pi [f(s) \nabla \log \pi(\cdot|s)] = 0$, we have

$$\mathbf{E}_\pi [\mathbf{E}_\pi[A] \cdot \nabla \log \pi] = 0,$$

$$\mathbf{E}_\pi [\log Z \cdot \nabla \log \pi] = 0.$$

On the one hand,

$$\begin{aligned} \mathbf{E}_\pi [(Q - V) \nabla \log \pi] &= \mathbf{E}_\pi [A \nabla \log \pi] - \mathbf{E}_\pi [\mathbf{E}_\pi[A] \cdot \nabla \log \pi] \\ &= \tau \mathbf{E}_\pi [\log \pi \nabla \log \pi] + \tau \mathbf{E}_\pi [\log Z \cdot \nabla \log \pi] \\ &= \tau \mathbf{E}_\pi [\log \pi \nabla \log \pi]. \end{aligned}$$

On the other hand,

$$\begin{aligned} \nabla \mathbf{H}[\pi] &= -\nabla \int_{\mathcal{A}} \pi_i \log \pi_i \\ &= -\int_{\mathcal{A}} \nabla \pi_i \cdot \log \pi_i - \int_{\mathcal{A}} \pi_i \nabla \log \pi_i \\ &= -\int_{\mathcal{A}} \pi_i \nabla \log \pi_i \cdot \log \pi_i - \int_{\mathcal{A}} \pi_i \frac{\nabla \pi_i}{\pi_i} \\ &= -\mathbf{E}_\pi [\log \pi \nabla \log \pi]. \end{aligned}$$

Hence, $\mathbf{E}_\pi [(Q - V) \nabla \log \pi] = -\tau \nabla \mathbf{H}[\pi]$. \square

Lemma 4. Let $v \in \mathbf{R}^{|\mathcal{A}|}$ to be a vector. Define $\pi(\tau) = \exp(v/\tau)/Z$, $Z = \int_{\mathcal{A}} \exp(v/\tau)$. Let Ω to be a probability measure supported on $[K, +\infty]$, then $f(\Omega) = \mathbf{E}_{\tau \sim \Omega} [\mathbf{E}_{\pi(\tau)}[v]]$ satisfies Lipschitz-1 condition with Wasserstein-1 metric.

Proof. Without loss of generality, we assume $v_1 \geq v_2 \geq \dots \geq v_{|\mathcal{A}|}$.

For any $\tau \in [0, +\infty)$, since

$$\pi(\tau) = \exp(v/\tau)/Z, \quad Z = \int_{\mathcal{A}} \exp(v/\tau),$$

we have

$$v = \tau \log \pi(\tau) + \tau \log Z.$$

Denote $\tilde{v}_j = v_j/\tau$.

Since

$$\frac{\partial \log \pi_i}{\partial \tilde{v}_j} = 1_{i=j} - \pi_j,$$

we have

$$\begin{aligned} \frac{\partial \log \pi_i}{\partial \tau} &= \sum_j \frac{\partial \log \pi_i}{\partial \tilde{v}_j} \cdot \frac{\partial \tilde{v}_j}{\partial \tau} \\ &= - \sum_j (1_{i=j} - \pi_j) \frac{v_j}{\tau^2} \\ &= - \frac{1}{\tau^2} (v_i - \sum_j \pi_j v_j) \\ &= - \frac{1}{\tau^2} (v_i - \mathbf{E}_\pi[v]). \end{aligned}$$

Therefore, we have

$$\begin{aligned} \frac{\partial \pi_i}{\partial \tau} &= \pi_i \frac{\partial \log \pi_i}{\partial \tau} \\ &= - \frac{\pi_i}{\tau^2} (v_i - \mathbf{E}_\pi[v]). \end{aligned}$$

Let $f(\tau) = v \cdot \pi(\tau)$, then

$$\frac{\partial f}{\partial \tau} = - \frac{1}{\tau^2} \sum_i v_i \pi_i (v_i - \mathbf{E}_\pi[v]).$$

Since $\sum_i \mathbf{E}_\pi[v] \pi_i (v_i - \mathbf{E}_\pi[v]) = 0$, we know

$$\begin{aligned} \frac{\partial f}{\partial \tau} &= - \frac{1}{\tau^2} \sum_i (v_i - \mathbf{E}_\pi[v]) \pi_i (v_i - \mathbf{E}_\pi[v]) \\ &= - \frac{1}{\tau^2} \sum_i \pi_i (v_i - \mathbf{E}_\pi[v])^2 \\ &= - \frac{1}{\tau^2} \mathbf{Var}_\pi[v]. \end{aligned}$$

It's obvious that

$$\left| \frac{\partial f}{\partial \tau} \right| \leq \frac{1}{K^2} |v_1 - v_{|\mathcal{A}|}|^2.$$

Hence, for any $\tau_1, \tau_2 \in [K, +\infty)$,

$$|v \cdot \pi(\tau_1) - v \cdot \pi(\tau_2)| \leq C |\tau_1 - \tau_2|.$$

Finally, for any $\gamma \in \Gamma(\Omega_1, \Omega_2)$ ⁸, we have

$$\begin{aligned} |\mathbf{E}_{\tau_1 \sim \Omega_1}[v \cdot \pi(\tau_1)] - \mathbf{E}_{\tau_2 \sim \Omega_2}[v \cdot \pi(\tau_2)]| &= \left| \int_{[K, +\infty) \times [K, +\infty)} (v \cdot \pi(\tau_1) - v \cdot \pi(\tau_2)) d\gamma(\tau_1, \tau_2) \right| \\ &\leq \int_{[K, +\infty) \times [K, +\infty)} |v \cdot \pi(\tau_1) - v \cdot \pi(\tau_2)| d\gamma(\tau_1, \tau_2) \\ &\leq C \int_{[K, +\infty) \times [K, +\infty)} |\tau_1 - \tau_2| d\gamma(\tau_1, \tau_2). \end{aligned}$$

⁸ $\Gamma(\Omega_1, \Omega_2)$ is the collection of all measures on $[K, +\infty) \times [K, +\infty)$ with marginals (Ω_1, Ω_2) .

Taking infimum over $\Gamma(\Omega_1, \Omega_2)$, we have

$$|\mathbf{E}_{\tau_1 \sim \Omega_1}[v \cdot \pi(\tau_1)] - \mathbf{E}_{\tau_2 \sim \Omega_2}[v \cdot \pi(\tau_2)]| \leq CW_1(\Omega_1, \Omega_2),$$

which proves that $f(\Omega) = \mathbf{E}_{\tau \sim \Omega}[\mathbf{E}_{\pi(\tau)}[v]]$ satisfies Lipschitz-1 condition with Wasserstein-1 metric. \square

Lemma 5. Define $\bar{A} = A - \mathbf{E}_{\pi}[A]$, $Q = \bar{A} + sg(V)$, then operator

$$\mathcal{F}(Q) \stackrel{def}{=} \mathbf{E}_{\mu,p}[Q(s_t, a_t)] + \sum_{k \geq 0} \gamma^k c_{[t+1:t+k-1]} \tilde{\rho}_{t,k} \delta_{t+k}^{DR} V$$

is a contraction mapping w.r.t. Q .

Remark. Note that $\mathcal{F}(Q)$ is exactly (7).

Since $Q = A + sg(V)$, the gradient of V is stopped when estimating Q , updating Q won't change V , which is equivalent to updating A . Without loss of generality, we assume V is fixed as V^* in the proof.

Proof. $\bar{A} = A - \mathbf{E}_{\pi}[A]$ shows $\mathbf{E}_{\pi}[\bar{A}] = 0$, which guarantees that no matter how we update A , we always have $\mathbf{E}_{\pi}[Q] = V^*$.

Based on above observations, define

$$\tilde{\mathcal{F}}(Q) \stackrel{def}{=} -\mathbf{E}_{\pi}[Q] + \mathcal{F}(Q).$$

It's obvious that we only need to prove $\tilde{\mathcal{F}}(Q)$ is a contraction mapping.

For brevity, we denote

$$Q_t = Q(s_t, a_t), A_t = A(s_t, a_t), V_t^* = V^*(s_t).$$

Notice that $\tilde{\rho}_{t,0} = 1$, similar to (Munos et al., 2016), we can rewrite $\tilde{\mathcal{F}}$ as

$$\begin{aligned} \tilde{\mathcal{F}}(Q) &= \mathbf{E}_{\mu,p}[A_t + \sum_{k \geq 0} \gamma^k c_{[t+1:t+k-1]} \tilde{\rho}_{t,k} \delta_{t+k}^{DR} V] \\ &= \mathbf{E}_{\mu,p}[-V_t^* + \sum_{k \geq 0} \gamma^k c_{[t+1:t+k-1]} \tilde{\rho}_{t,k} r_{t+k} + \sum_{k \geq 0} \gamma^{k+1} c_{[t+1:t+k-1]} \Delta_k], \end{aligned} \quad (19)$$

where

$$\Delta_k = \mathbf{E}_{\mu,p} [\tilde{\rho}_{t,k} V_{t+k+1}^* - c_{t+k} \tilde{\rho}_{t,k+1} Q_{t+k+1} | \mathcal{F}_{t+k}].^9 \quad (20)$$

By definition of Q ,

$$\mathbf{E}_{\mu,p}[V_{t+k+1}^* | \mathcal{F}_{t+k}] = \mathbf{E}_{\mu,p}[\mathbf{E}_{\pi}[Q_{t+k+1} | \mathcal{F}_{t+k+1}] | \mathcal{F}_{t+k}],$$

we can rewrite (20) as

$$\Delta_k = \mathbf{E}_{\mu,p}[(\tilde{\rho}_{t,k} \frac{\pi_{t+k+1}}{\mu_{t+k+1}} - c_{t+k} \tilde{\rho}_{t,k+1}) Q_{t+k+1} | \mathcal{F}_{t+k}]. \quad (21)$$

For any $Q^1 = A^1 + sg(V^*)$, $Q^2 = A^2 + sg(V^*)$, since

$$\mathbf{E}_{\mu,p}[(\tilde{\rho}_{t,k} \frac{\pi_{t+k+1}}{\mu_{t+k+1}} - c_{t+k} \tilde{\rho}_{t,k+1}) | \mathcal{F}_{t+k}] \geq 0,$$

by (19) (21), we have

$$\|\tilde{\mathcal{F}}(Q^1) - \tilde{\mathcal{F}}(Q^2)\| \leq C \|Q^1 - Q^2\|,$$

⁹ \mathcal{F} represents filtration.

where

$$\begin{aligned}
C &= \mathbf{E}_{\mu,p} \left[\sum_{k \geq 0} \gamma^{k+1} c_{[t+1:t+k-1]} (\tilde{\rho}_{t,k} \frac{\pi_{t+k+1}}{\mu_{t+k+1}} - c_{t+k} \tilde{\rho}_{t,k+1}) \right] \\
&= \mathbf{E}_{\mu,p} \left[1 - 1 + \sum_{k \geq 0} \gamma^{k+1} c_{[t+1:t+k-1]} (\tilde{\rho}_{t,k} - c_{t+k} \tilde{\rho}_{t,k+1}) \right] \\
&= 1 - (1 - \gamma) \mathbf{E}_{\mu,p} \left[\sum_{k \geq 0} \gamma^k c_{[t+1:t+k-1]} \tilde{\rho}_{t,k} \right] \\
&\leq 1 - (1 - \gamma) < 1.
\end{aligned}$$

Hence, $\tilde{\mathcal{F}}(Q)$ is a contraction mapping and converges to some fixed function, which we denote as A^* . So $\mathcal{S}(Q)$ is also a contraction mapping and converges to $A^* + V^*$. \square

Lemma 6. Define $Q = A + sg(V)$ with $\mathbf{E}_\pi[A] = 0$, then operator

$$\mathcal{S}(V) \stackrel{def}{=} \mathbf{E}_{\mu,p} [V(s_t) + \sum_{k \geq 0} \gamma^k c_{[t:t+k-1]} \rho_{t,k} \delta_{t+k}^{DR} V]$$

is a contraction mapping w.r.t. V .

Remark. Note that $\mathcal{S}(V)$ is exactly (6).

Proof. Same as Lemma 5, we can get

$$\Delta_k = \mathbf{E}_{\mu,p} [(\rho_{t+k} - c_{t+k} \rho_{t+k+1}) V_{t+k+1} - c_{t+k} \rho_{t+k+1} A_{t+k+1}^* | \mathcal{F}_{t+k}],$$

so we have

$$\Delta_k^1 - \Delta_k^2 = \mathbf{E}_{\mu,p} [(\rho_{t+k} - c_{t+k} \rho_{t+k+1}) \cdot (V_{t+k+1}^1 - V_{t+k+1}^2) | \mathcal{F}_{t+k}].$$

The proof attributes to (Espenholt et al., 2018). \square

Theorem 1. Define $\bar{A} = A - \mathbf{E}_\pi[A]$, $Q = \bar{A} + sg(V)$. Define

$$\mathcal{T}(Q) \stackrel{def}{=} \mathbf{E}_{\mu,p} [Q(s_t, a_t) + \sum_{k \geq 0} \gamma^k c_{[t+1:t+k-1]} \tilde{\rho}_{t,k} \delta_{t+k}^{DR} V],$$

$$\mathcal{S}(V) \stackrel{def}{=} \mathbf{E}_{\mu,p} [V(s_t) + \sum_{k \geq 0} \gamma^k c_{[t:t+k-1]} \rho_{t,k} \delta_{t+k}^{DR} V],$$

$$\mathcal{U}(Q, V) = (\mathcal{T}(Q) - \mathbf{E}_\pi[Q] + \mathcal{S}(V), \mathcal{S}(V)),$$

$$\mathcal{U}^{(n)}(Q, V) = \mathcal{U}(\mathcal{U}^{(n-1)}(Q, V)),$$

then $\mathcal{U}^{(n)}(Q, V) \rightarrow (Q^{\tilde{\pi}}, V^{\tilde{\pi}})$ that corresponds to

$$\tilde{\pi}(a|s) = \frac{\min \{\bar{\rho}\mu(a|s), \pi(a|s)\}}{\sum_{b \in \mathcal{A}} \min \{\bar{\rho}\mu(b|s), \pi(b|s)\}}.$$

as $n \rightarrow +\infty$.

Remark. $\mathcal{T}(Q) - \mathbf{E}_\pi[Q] + \mathcal{S}(V)$ is **exactly** how Q is updated at training time. Since $Q = A + sg(V)$, if we apply gradient ascent on Q and V in directions (9) respectively, change of Q comes from two aspects. One comes from $\nabla Q(\theta)$, which changes A , the other comes from $\nabla V(\theta)$, which changes V . Because the gradient of V is stopped when estimating Q , the latter is captured by "minus old baseline, add new baseline", which is $-\mathbf{E}_\pi[Q] + \mathcal{S}(V)$ in Theorem 1.

Proof. Define

$$\tilde{\mathcal{F}}(Q) = -\mathbf{E}_\pi[Q] + \mathcal{T}(Q),$$

$$\tilde{\mathcal{U}}(Q, V) = (\tilde{\mathcal{F}}(Q), \mathcal{S}(V)),$$

$$\tilde{\mathcal{U}}^{(n)}(Q, V) = \tilde{\mathcal{U}}(\tilde{\mathcal{U}}^{(n-1)}(Q, V)).$$

By Lemma 5, $\tilde{\mathcal{F}}^{(n)}(Q)$ converges to some A^* as $n \rightarrow \infty$. This process won't influence the estimation of V as the gradient of V is stopped when estimating Q . According to the proof, A^* doesn't depend

on V .

By Lemma 6, $\mathcal{S}^{(n)}(V)$ converges to some V^* as $n \rightarrow \infty$.

Hence, we have

$$\tilde{\mathcal{U}}^{(n)}(Q, V) \rightarrow (A^*, V^*) \text{ as } n \rightarrow +\infty.$$

By definition,

$$\mathcal{U}(Q, V) = (\tilde{\mathcal{T}}(Q) + \mathcal{S}(V), \mathcal{S}(V)),$$

we can regard $\tilde{\mathcal{T}}(Q) + \mathcal{S}(V)$ as Q and regard $\mathcal{S}(V)$ as V , then

$$\begin{aligned} \mathcal{U}^{(2)}(Q, V) &= \mathcal{U}(\tilde{\mathcal{T}}(Q) + \mathcal{S}(V), \mathcal{S}(V)) \\ &= (\mathcal{T}(\tilde{\mathcal{T}}(Q) + \mathcal{S}(V)) - \mathcal{S}(V) + \mathcal{S}^{(2)}(V), \mathcal{S}^{(2)}(V)) \\ &= (\tilde{\mathcal{T}}^{(2)}(Q) + \mathcal{S}^{(2)}(V), \mathcal{S}^{(2)}(V)). \end{aligned}$$

By induction,

$$\begin{aligned} \mathcal{U}^{(n)}(Q, V) &= (\tilde{\mathcal{T}}^{(n)}(Q) + \mathcal{S}^{(n)}(V), \mathcal{S}^{(n)}(V)) \\ &\rightarrow (A^* + V^*, V^*) \text{ as } n \rightarrow +\infty. \end{aligned}$$

Same as (Espeholt et al., 2018),

$$\tilde{\pi}(a|s) = \frac{\min\{\bar{\rho}\mu(a|s), \pi(a|s)\}}{\sum_{b \in \mathcal{A}} \min\{\bar{\rho}\mu(b|s), \pi(b|s)\}}.$$

is the policy s.t. the Bellman equation holds, which is

$$\mathbf{E}_\mu[\rho_t(r_t + \gamma V_{t+1} - V_t) | \mathcal{F}_t] = 0,$$

and $\mathcal{U}(Q^{\tilde{\pi}}, V^{\tilde{\pi}}) = (Q^{\tilde{\pi}}, V^{\tilde{\pi}})$.

So we have $(A^* + V^*, V^*) = (Q^{\tilde{\pi}}, V^{\tilde{\pi}})$. □

D Hyperparameters

Parameter	Value
Image Size	(84, 84)
Grayscale	Yes
Num. Action Repeats	4
Num. Frame Stacks	4
Action Space	Full
End of Episode When Life Lost	No
Num. States	200M
Sample Reuse	2
Num. Environments	160
Reward Shape	$\log(\text{abs}(r) + 1.0) \cdot (2 \cdot 1_{\{r \geq 0\}} - 1_{\{r < 0\}})$
Reward Clip	No
Intrinsic Reward	No
Random No-ops	30
Burn-in	40
Seq-length	80
Burn-in Stored Recurrent State	Yes
Bootstrap	Yes
Batch size	64
Discount (γ)	0.997
V -loss Scaling (ξ)	1.0
Q -loss Scaling (α)	10.0
π -loss Scaling (β)	10.0
Entropy Regularization	No
DR-Trace Importance Sampling Clip \bar{c}	1.05
DR-Trace Importance Sampling Clip $\bar{\rho}$	1.05
Backbone	IMPALA,deep
LSTM Units	256
Optimizer	Adam Weight Decay
Weight Decay Rate	0.01
Weight Decay Schedule	Anneal linearly to 0
Learning Rate	5e-4
Warmup Steps	4000
Learning Rate Schedule	Anneal linearly to 0
AdamW β_1	0.9
AdamW β_2	0.98
AdamW ϵ	1e-6
AdamW Clip Norm	50.0
Auxiliary Forward Dynamic Task	Yes
Auxiliary Inverse Dynamic Task	Yes
Learner Push Model Every n Steps	25
Actor Pull Model Every n Steps	64
Num. Bandits	7
Bandit Learning Rate	Uniform([0.05, 0.1, 0.2])
Bandit Tiling Width	Uniform([1, 2, 3])
Num. Bandit Candidates	7
Bandit Value Normalization	Yes
Bandit UCB Scaling	1.0
Bandit Search Range for $1/\tau$	[0.0, 50.0]

Table 2: Hyperparameters for Atari Experiments.

E Ablation Study

The details of ablation changes are listed in Table E. The evaluation curves are attached in Figure 4.

Ablation	Change
CASA-B	N/A
<i>no_stop_pi</i>	$\bar{A} = A - \mathbf{E}_\pi[A] = A - sg(\pi) \cdot A \Rightarrow \bar{A} = A - \pi \cdot A$
<i>no_stop_v</i>	$Q = \bar{A} + sg(V) \Rightarrow Q = \bar{A} + V$
<i>no_drtrace</i>	$vs = V_t + \sum_{k \geq 0} \gamma^k c_{[t:t+k-1]} \rho_{t+k} (r_{t+k} + \gamma V_{t+k+1} - Q_{t+k})$ $\Rightarrow vs = V(s_t) + \sum_{k \geq 0} \gamma^k c_{[t:t+k-1]} \rho_{t+k} (r_{t+k} + \gamma V_{t+k+1} - V_{t+k}),$ $qs = Q(s_t, a_t) + \sum_{k \geq 0} \gamma^k c_{[t+1:t+k-1]} \tilde{\rho}_{t,k} (r_{t+k} + \gamma V_{t+k+1} - Q_{t+k})$ $\Rightarrow qs = Q(s_t, a_t) + \sum_{k \geq 0} \gamma^k c_{[t+1:t+k-1]} \tilde{\rho}_{t,k} (r_{t+k} + \gamma Q_{t+k+1} - Q_{t+k})$
<i>random_scaling</i>	Q-loss Scaling $\alpha = 10.0 \Rightarrow \alpha \sim Uniform([0.0, 20.0])$ for every sample of every batch, π -loss Scaling $\beta = 10.0 \Rightarrow \beta \sim Uniform([0.0, 20.0])$ for every sample of every batch
<i>trainable_tau</i>	τ is treated as a trainable variable rather than an input in $\pi = P(A/\tau)$, BVA is also disabled
<i>no_bva</i>	BVA is not updated, so τ is sampled from a fixed distribution Ω

Table 3: Ablation Changes. The baseline of these ablation changes is **original CASA-B**. Except for the changes listed in the table, there is no other change of CASA-B in each ablation case.

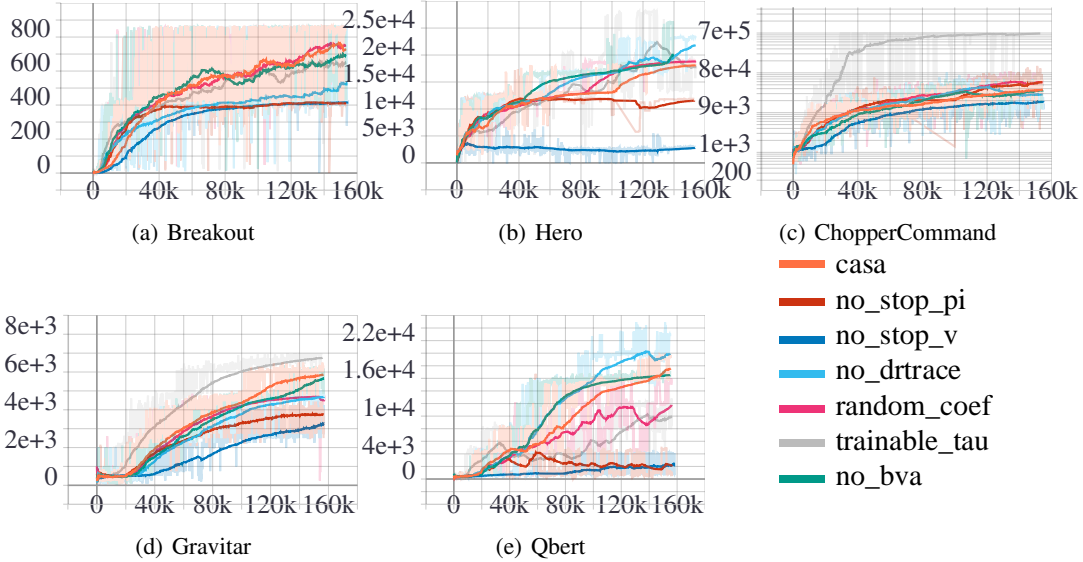


Figure 4: Evaluation Return Curves. The labels are identical to the ablation changes in Table E. For ease of comparison, all curves are smoothed with rate 0.99. ChopperCommand’s y-axes is in a log scale, others’ are in a linear scale.

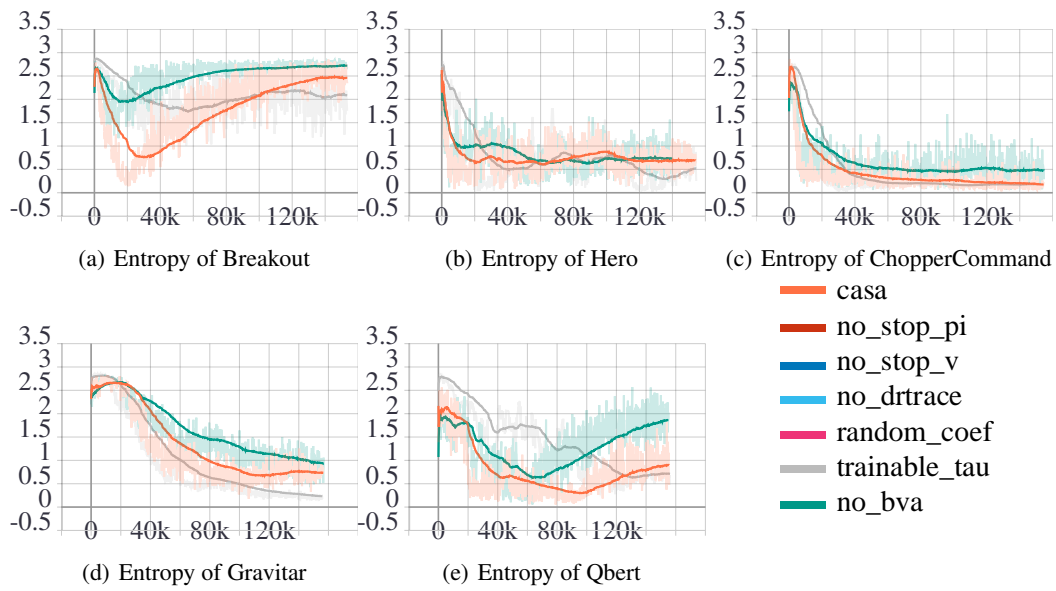


Figure 5: Entropy of Ablation Study. The labels are identical to the ablation changes Table E. We only draw entropy curves of CASA-B, *trainable_tau* and *no_bva*, because theirs entropy curves show very same trend in different games. In general, the entropy curve of *no_bva* is above CASA-B along the whole training process. The entropy curve of *trainable_tau* drops slower than CASA-B’s. It’s above CASA-B’s at the beginning of training for a period, but it finally drops below CASA-B’s at the end of training.

F Atari Results

F.1 Atari Games Table of Scores Based on Human Average Records

Random scores and average human’s scores are from (Badia et al., 2020a). Rainbow’s scores are from (Hessel et al., 2017). IMPALA’s scores are from (Espeholt et al., 2018). LASER’s scores are from (Schmitt et al., 2020), no sweep at 200M. As there are many versions of R2D2 and NGU, we use original papers’. R2D2’s scores are from (Kapturowski et al., 2018). NGU’s scores are from (Badia et al., 2020b). Agent57’s scores are from (Badia et al., 2020a).

Games	RND	HUMAN	RAINBOW	HNS(%)	IMPALA	HNS(%)	LASER	HNS(%)	OURS	HNS(%)
Scale			200M		200M		200M		200M	
alien	227.8	7127.8	9491.7	134.26	15962.1	228.03	35565.9	512.15	10641	150.92
amidar	5.8	1719.5	5131.2	299.08	1554.79	90.39	1829.2	106.4	653.9	37.82
assault	222.4	742	14198.5	2689.78	19148.47	3642.43	21560.4	4106.62	36251	6933.91
asterix	210	8503.3	428200	5160.67	300732	3623.67	240090	2892.46	851210	10261.30
asteroids	719	47388.7	2712.8	4.27	108590.05	231.14	213025	454.91	759170	1625.15
atlantis	12850	29028.1	826660	5030.32	849967.5	5174.39	841200	5120.19	3670700	22609.89
bank heist	14.2	753.1	1358	181.86	1223.15	163.61	569.4	75.14	1381	184.98
battle zone	236	37187.5	62010	167.18	20885	55.88	64953.3	175.14	130410	352.28
beam rider	363.9	16926.5	16850.2	99.54	32463.47	193.81	90881.6	546.52	104030	625.90
berzerk	123.7	2630.4	2545.6	96.62	1852.7	68.98	25579.5	1015.51	1222	43.81
bowling	23.1	160.7	30	5.01	59.92	26.76	48.3	18.31	176.4	111.41
boxing	0.1	12.1	99.6	829.17	99.96	832.17	100	832.5	99.9	831.67
breakout	1.7	30.5	417.5	1443.75	787.34	2727.92	747.9	2590.97	696	2410.76
centipede	2090.9	12017	8167.3	61.22	11049.75	90.26	292792	2928.65	38938	371.21
chopper command	811	7387.8	16654	240.89	28255	417.29	761699	11569.27	41495	618.60
crazy climber	10780.5	36829.4	168788.5	630.80	136950	503.69	167820	626.93	157250	584.73
defender	2874.5	18688.9	55105	330.27	185203	1152.93	336953	2112.50	837750	5279.21
demon attack	152.1	1971	111185	6104.40	132826.98	7294.24	133530	7332.89	549450	30199.46
double dunk	-18.6	-16.4	-0.3	831.82	-0.33	830.45	14	1481.82	23	1890.91
enduro	0	860.5	2125.9	247.05	0	0.00	0	0.00	14317	1663.80
fishing derby	-91.7	-38.8	31.3	232.51	44.85	258.13	45.2	258.79	48.8	265.60
freeway	0	29.6	34	114.86	0	0.00	0	0.00	33.7	113.85
frostbite	65.2	4334.7	9590.5	223.10	317.75	5.92	5083.5	117.54	8102	188.24
gopher	257.6	2412.5	70354.6	3252.91	66782.3	3087.14	114820.7	5316.40	454150	21063.27
gravitar	173	3351.4	1419.3	39.21	359.5	5.87	1106.2	29.36	6150	188.05
hero	1027	30826.4	55887.4	184.10	33730.55	109.75	31628.7	102.69	17655	55.80
ice hockey	-11.2	0.9	1.1	101.65	3.48	121.32	17.4	236.36	-8.1	25.62
jamesbond	29	302.8	19809	72.24	601.5	209.09	37999.8	13868.08	567020	207082.18
kangaroo	52	3035	14637.5	488.05	1632	52.97	14308	477.91	14286	477.17
krull	1598	2665.5	8741.5	669.18	8147.4	613.53	9387.5	729.70	11104	890.49
kung fu master	258.5	22736.3	52181	230.99	43375.5	191.82	607443	2701.26	1270800	5652.43
montezuma revenge	0	4753.3	384	8.08	0	0.00	0.3	0.01	2528	53.18
ms pacman	307.3	6951.6	5380.4	76.35	7342.32	105.88	6565.5	94.19	4296	60.03
name this game	2292.3	8049	13136	188.37	21537.2	334.30	26219.5	415.64	30037	481.95
phoenix	761.5	7242.6	108529	1662.80	210996.45	3243.82	519304	8000.84	597580	9208.60
pitfall	-229.4	6463.7	0	3.43	-1.66	3.40	-0.6	3.42	-21.8	3.10
pong	-20.7	14.6	20.9	117.85	20.98	118.07	21	118.13	21	118.13
private eye	24.9	69571.3	4234	6.05	98.5	0.11	96.3	0.10	15095	21.67
qbert	163.9	13455.0	33817.5	253.20	351200.12	2641.14	21449.6	160.15	19091	142.40
riverraid	1338.5	17118.0	22920.8	136.77	29608.05	179.15	40362.7	247.31	17081	99.77
road runner	11.5	7845	62041	791.85	57121	729.04	45289	578.00	57102	728.80
robotank	2.2	11.9	61.4	610.31	12.96	110.93	62.1	617.53	69.7	695.88
seaquest	68.4	42054.7	15898.9	37.70	1753.2	4.01	2890.3	6.72	2728	6.33
skiing	-17098	-4336.9	-12957.8	32.44	-10180.38	54.21	-29968.4	-100.86	-9327	60.90
solaris	1236.3	12326.7	3560.3	20.96	2365	10.18	2273.5	9.35	3653	21.79
space invaders	148	1668.7	18789	1225.82	43595.78	2857.09	51037.4	3346.45	105810	6948.25
star gunner	664	10250	127029	1318.22	200625	2085.97	321528	3347.21	358650	3734.47
surround	-10	6.5	9.7	119.39	7.56	106.42	8.4	111.52	-9.8	1.21
tennis	-23.8	-8.3	0	153.55	0.55	157.10	12.2	232.26	23.7	306.45
time pilot	3568	5229.2	12926	563.36	48481.5	2703.84	105316	6125.34	150930	8871.35
tutankham	11.4	167.6	241	146.99	292.11	179.71	278.9	171.25	380.3	236.17
up n down	533.4	11693.2	125755	1122.08	332546.75	2975.08	345727	3093.19	907170	8124.13
venture	0	1187.5	5.5	0.46	0	0.00	0	0.00	1969	165.81
video pinball	0	17667.9	533936.5	3022.07	572898.27	3242.59	511835	2896.98	673840	3813.92
wizard of wor	563.5	4756.5	17862.5	412.57	9157.5	204.96	29059.3	679.60	21325	495.15
yars revenge	3092.9	54576.9	102557	193.19	84231.14	157.60	166292.3	316.99	84684	158.48
zaxxon	32.5	9173.3	22209.5	242.62	32935.5	359.96	41118	449.47	62133	679.38
MEAN HNS(%)	0.00	100.00		873.97		957.34		1741.36		6456.63
MEDIAN HNS(%)	0.00	100.00		230.99		191.82		454.91		477.17

Games	R2D2	HNS(%)	NGU	HNS(%)	AGENT57	HNS(%)	OURS	HNS(%)
Scale	10B		35B		100B		200M	
alien	109038.4	1576.97	248100	3592.35	297638.17	4310.30	10641	150.92
amidar	27751.24	1619.04	17800	1038.35	29660.08	1730.42	653.9	37.82
assault	90526.44	17379.53	34800	6654.66	67212.67	12892.66	36251	6933.91
asterix	999080	12044.30	950700	11460.94	991384.42	11951.51	851210	10261.30
asteroids	265861.2	568.12	230500	492.36	150854.61	321.70	759170	1625.15
atlantis	1576068	9662.56	1653600	10141.80	1528841.76	9370.64	3670700	22609.89
bank heist	46285.6	6262.20	17400	2352.93	23071.5	3120.49	1381	184.98
battle zone	513360	1388.64	691700	1871.27	934134.88	2527.36	130410	352.28
beam rider	128236.08	772.05	63600	381.80	300509.8	1812.19	104030	625.90
berzerk	34134.8	1356.81	36200	1439.19	61507.83	2448.80	1222	43.81
bowling	196.36	125.92	211.9	137.21	251.18	165.76	176.4	111.41
boxing	99.16	825.50	99.7	830.00	100	832.50	99.9	831.67
breakout	795.36	2755.76	559.2	1935.76	790.4	2738.54	696	2410.76
centipede	532921.84	5347.83	577800	5799.95	412847.86	4138.15	38938	371.21
chopper command	960648	14594.29	999900	15191.11	999900	15191.11	41495	618.60
crazy climber	312768	1205.59	313400	1208.11	565909.85	2216.18	157250	584.73
defender	562106	3536.22	664100	4181.16	677642.78	4266.80	837750	5279.21
demon attack	143664.6	7890.07	143500	7881.02	143161.44	7862.41	549450	30199.46
double dunk	23.12	1896.36	-14.1	204.55	23.93	1933.18	23	1890.91
enduro	2376.68	276.20	2000	232.42	2367.71	275.16	14317	1663.80
fishing derby	81.96	328.28	32	233.84	86.97	337.75	48.8	265.60
freeway	34	114.86	28.5	96.28	32.59	110.10	33.7	113.85
frostbite	11238.4	261.70	206400	4832.76	541280.88	12676.32	8102	188.24
gopher	122196	5658.66	113400	5250.47	117777.08	5453.59	454150	21063.27
gravitar	6750	206.93	14200	441/32	19213.96	599.07	6150	188.05
hero	37030.4	120.82	69400	229.44	114736.26	381.58	17655	55.80
ice hockey	71.56	683.97	-4.1	58.68	63.64	618.51	-8.1	25.62
jamesbond	23266	8486.85	26600	9704.53	135784.96	49582.16	567020	207082.18
kangaroo	14112	471.34	35100	1174.92	24034.16	803.96	14286	477.17
krull	145284.8	13460.12	127400	11784.73	251997.31	23456.61	11104	890.49
kung fu master	200176	889.40	212100	942.45	206845.82	919.07	1270800	5652.43
montezuma revenge	2504	52.68	10400	218.80	9352.01	196.75	2528	53.18
ms pacman	29928.2	445.81	40800	609.44	63994.44	958.52	4296	60.03
name this game	45214.8	745.61	23900	375.35	54386.77	904.94	30037	481.95
phoenix	811621.6	125.11	959100	14786.66	908264.15	14002.29	597580	9208.60
pitfall	0	3.43	7800	119.97	18756.01	283.66	-21.8	3.10
pong	21	118.13	19.6	114.16	20.67	117.20	21	118.13
private eye	300	0.40	100000	143.75	79716.46	114.59	15095	21.67
qbert	161000	1210.10	451900	3398.79	580328.14	4365.06	19091	142.40
riverraid	34076.4	207.47	36700	224.10	63318.67	392.79	17081	99.77
road runner	498660	6365.59	128600	1641.52	243025.8	3102.24	57102	728.80
robotank	132.4	1342.27	9.1	71.13	127.32	1289.90	69.7	695.88
seaquest	999991.84	2381.55	1000000	2381.57	999997.63	2381.56	2728	6.33
skiing	-29970.32	-100.87	-22977.9	-46.08	-4202.6	101.05	-9327	60.90
solaris	4198.4	26.71	4700	31.23	44199.93	387.39	3653	21.79
space invaders	55889	3665.48	43400	2844.22	48680.86	3191.48	105810	6948.25
star gunner	521728	5435.68	414600	4318.13	839573.53	8751.40	358650	3734.47
surround	9.96	120.97	-9.6	2.42	9.5	118.18	-9.8	1.21
tennis	24	308.39	10.2	219.35	23.84	307.35	23.7	306.45
time pilot	348932	20791.28	344700	20536.51	405425.31	24192.24	150930	8871.35
tutankham	393.64	244.71	191.1	115.04	2354.91	1500.33	380.3	236.17
up n down	542918.8	4860.17	620100	5551.77	623805.73	5584.98	907170	8124.13
venture	1992	167.75	1700	143.16	2623.71	220.94	1969	165.81
video pinball	483569.72	2737.00	965300	5463.58	992340.74	5616.63	673840	3813.92
wizard of wor	133264	3164.81	106200	2519.35	157306.41	3738.20	21325	495.15
yars revenge	918854.32	1778.73	986000	1909.15	998532.37	1933.49	84684	158.48
zaxxon	181372	1983.85	111100	1215.07	249808.9	2732.54	62133	679.38
MEAN HNS(%)		3374.31		3169.90		4763.69		6456.63
MEDIAN HNS(%)		1342.27		1208.11		1933.49		477.17

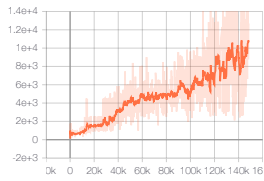
F.2 Atari Games Table of Scores Based on SABER

Games	RND	HWR	RAINBOW SABER(%)	IMPALA SABER(%)	LASER SABER(%)	OURS SABER(%)				
Scale	200M		200M	200M	200M	200M				
alien	227.8	251916	9491.7	3.68	15962.1	6.25	976.51	14.04	10641	4.14
amidar	5.8	104159	5131.2	4.92	1554.79	1.49	1829.2	1.75	653.9	0.62
assault	222.4	8647	14198.5	165.90	19148.47	200.00	21560.4	200.00	36251	200.00
asterix	210	1000000	428200	42.81	300732	30.06	240090	23.99	851210	85.12
asteroids	719	10506650	2712.8	0.02	108590.05	1.03	213025	2.02	759170	7.22
atlantis	12850	10604840	826660	7.68	849967.5	7.90	841200	7.82	3670700	34.53
bank heist	14.2	82058	1358	1.64	1223.15	1.47	569.4	0.68	1381	1.67
battle zone	236	801000	62010	7.71	20885	2.58	64953.3	8.08	130410	16.26
beam rider	363.9	999999	16850.2	1.65	32463.47	3.21	90881.6	9.06	104030	10.37
berzerk	123.7	1057940	2545.6	0.23	1852.7	0.16	25579.5	2.41	1222	0.10
bowling	23.1	300	30	2.49	59.92	13.30	48.3	9.10	176.4	55.36
boxing	0.1	100	99.6	99.60	99.96	99.96	100	100.00	99.9	99.90
breakout	1.7	864	417.5	48.22	787.34	91.11	747.9	86.54	696	80.52
centipede	2090.9	1301709	8167.3	0.47	11049.75	0.69	292792	22.37	38938	2.84
chopper command	811	999999	16654	1.59	28255	2.75	761699	76.15	41495	4.07
crazy climber	10780.5	219900	168788.5	75.56	136950	60.33	167820	75.10	157250	70.04
defender	2874.5	6010500	55105	0.87	185203	3.03	336953	5.56	837750	13.90
demon attack	152.1	1556345	111185	7.13	132826.98	8.53	133530	8.57	549450	35.30
double dunk	-18.6	21	-0.3	46.21	-0.33	46.14	14	82.32	23	105.05
enduro	0	9500	2125.9	22.38	0	0.00	0	0.00	14317	150.71
fishing derby	-91.7	71	31.3	75.60	44.85	83.93	45.2	84.14	48.8	86.36
freeway	0	38	34	89.47	0	0.00	0	0.00	33.7	88.68
frostbite	65.2	454830	9590.5	2.09	317.75	0.06	5083.5	1.10	8102	1.77
gopher	257.6	355040	70354.6	19.76	66782.3	18.75	114820.7	32.29	454150	127.94
gravitar	173	162850	1419.3	0.77	359.5	0.11	1106.2	0.57	6150	3.67
hero	1027	1000000	55887.4	5.49	33730.55	3.27	31628.7	3.06	17655	1.66
ice hockey	-11.2	36	1.1	26.06	3.48	31.10	17.4	60.59	-8.1	6.57
jamesbond	29	45550	19809	43.45	601.5	1.26	37999.8	83.41	567020	200.00
kangaroo	52	1424600	14637.5	1.02	1632	0.11	14308	1.00	14286	1.00
krull	1598	104100	8741.5	6.97	8147.4	6.39	9387.5	7.60	11104	9.27
kung fu master	258.5	1000000	52181	5.19	43375.5	4.31	607443	60.73	1270800	127.09
montezuma revenge	0	1219200	384	0.03	0	0.00	0.3	0.00	2528	0.21
ms pacman	307.3	290090	5380.4	1.75	7342.32	2.43	6565.5	2.16	4296	1.38
name this game	2292.3	25220	13136	47.30	21537.2	83.94	26219.5	104.36	30037	121.01
phoenix	761.5	4014440	108529	2.69	210996.45	5.24	519304	12.92	597580	14.87
pitfall	-229.4	114000	0	0.20	-1.66	0.20	-0.6	0.20	-21.8	0.18
pong	-20.7	21	20.9	99.76	20.98	99.95	21	100.00	21	100.00
private eye	24.9	101800	4234	4.14	98.5	0.07	96.3	0.07	15095	14.81
qbert	163.9	2400000	33817.5	1.40	351200.12	14.63	21449.6	0.89	19091	0.79
riverraid	1338.5	1000000	22920.8	2.16	29608.05	2.83	40362.7	3.91	17081	1.58
road runner	11.5	2038100	62041	3.04	57121	2.80	45289	2.22	57102	2.80
robotank	2.2	76	61.4	80.22	12.96	14.58	62.1	81.17	69.7	91.46
seaquest	68.4	999999	15898.9	1.58	1753.2	0.17	2890.3	0.28	2728	0.27
skiing	-17098	-3272	-12957.8	29.95	-10180.38	50.03	-29968.4	-93.09	-9327	56.21
solaris	1236.3	111420	3560.3	2.11	2365	1.02	2273.5	0.94	3653	2.19
space invaders	148	621535	18789	3.00	43595.78	6.99	51037.4	8.19	105810	17.00
star gunner	664	77400	127029	164.67	200625	200.00	321528	418.14	358650	200.00
surround	-10	9.6	9.7	100.51	7.56	89.59	8.4	93.88	-9.8	1.02
tennis	-23.8	21	0	53.13	0.55	54.35	12.2	80.36	23.7	106.03
time pilot	3568	65300	12926	15.16	48481.5	72.76	105316	164.82	150930	200.00
tutankham	11.4	5384	241	4.27	292.11	5.22	278.9	4.98	380.3	6.87
up n down	533.4	82840	125755	152.14	332546.75	403.39	345727	200.00	907170	200.00
venture	0	38900	5.5	0.01	0	0.00	0	0.00	1969	5.06
video pinball	0	89218328	533936.5	0.60	572898.27	0.64	511835	0.57	673840	0.76
wizard of wor	563.5	395300	17862.5	4.38	9157.5	2.18	29059.3	7.22	21325	5.26
yars revenge	3092.9	15000105	102557	0.66	84231.14	0.54	166292.3	1.09	84684	0.54
zaxxon	32.5	83700	22209.5	26.51	32935.5	39.33	41118	49.11	62133	74.22
MEAN SABER(%)	0.00	100.00		28.39		29.45		36.78		50.11
MEDIAN SABER(%)	0.00	100.00		4.92		4.31		8.08		13.90

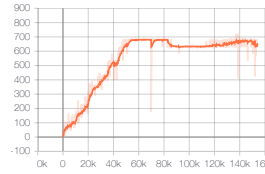
Table 4: Score table of SOTA 200M model-free algorithms on SABER.

Games	R2D2	SABER(%)	NGU	SABER(%)	AGENT57	SABER(%)	OURS	SABER(%)
Scale	10B		35B		100B		200M	
alien	109038.4	43.23	248100	98.48	297638.17	118.17	10641	4.14
amidar	27751.24	26.64	17800	17.08	29660.08	28.47	653.9	0.62
assault	90526.44	200.00	34800	410.44	67212.67	200.00	36251	200.00
asterix	999080	99.91	950700	95.07	991384.42	99.14	851210	85.12
asteroids	265861.2	2.52	230500	2.19	150854.61	1.43	759170	7.22
atlantis	1576068	14.76	1653600	15.49	1528841.76	14.31	3670700	34.53
bank heist	46285.6	56.40	17400	21.19	23071.5	28.10	1381	1.67
battle zone	513360	64.08	691700	86.35	934134.88	116.63	130410	16.26
beam rider	128236.08	12.79	63600	6.33	300509.8	30.03	104030	10.37
berzerk	34134.8	3.22	36200	3.41	61507.83	5.80	1222	0.10
bowling	196.36	62.57	211.9	68.18	251.18	82.37	176.4	55.36
boxing	99.16	99.16	99.7	99.70	100	100.00	99.9	99.90
breakout	795.36	92.04	559.2	64.65	790.4	91.46	696	80.52
centipede	532921.84	40.85	577800	44.30	412847.86	31.61	38938	2.84
chopper command	960648	96.06	999900	99.99	999900	99.99	41495	4.07
crazy climber	312768	144.41	313400	144.71	565909.85	200.00	157250	70.04
defender	562106	9.31	664100	11.01	677642.78	11.23	837750	13.90
demon attack	143664.6	9.22	143500	9.21	143161.44	9.19	549450	35.30
double dunk	23.12	105.35	-14.1	11.36	23.93	107.40	23	105.05
enduro	2376.68	25.02	2000	21.05	2367.71	24.92	14317	150.71
fishing derby	81.96	106.74	32	76.03	86.97	109.82	48.8	86.36
freeway	34	89.47	28.5	75.00	32.59	85.76	33.7	88.68
frostbite	11238.4	2.46	206400	45.37	541280.88	119.01	8102	1.77
gopher	122196	34.37	113400	31.89	117777.08	33.12	454150	127.94
gravitar	6750	4.04	14200	8.62	19213.96	11.70	6150	3.67
hero	37030.4	3.60	69400	6.84	114736.26	11.38	17655	1.66
ice hockey	71.56	175.34	-4.1	15.04	63.64	158.56	-8.1	6.57
jamesbond	23266	51.05	26600	58.37	135784.96	200.00	567020	200.00
kangaroo	14112	0.99	35100	2.46	24034.16	1.68	14286	1.00
krull	145284.8	140.18	127400	122.73	251997.31	200.00	11104	9.27
kung fu master	200176	20.00	212100	21.19	206845.82	20.66	1270800	127.09
montezuma revenge	2504	0.21	10400	0.85	9352.01	0.77	2528	0.21
ms pacman	29928.2	10.22	40800	13.97	63994.44	21.98	4296	1.38
name this game	45214.8	187.21	23900	94.24	54386.77	200.00	30037	121.01
phoenix	811621.6	20.20	959100	23.88	908264.15	22.61	597580	14.87
pitfall	0	0.20	7800	7.03	18756.01	16.62	-21.8	0.18
pong	21	100.00	19.6	96.64	20.67	99.21	21	100.00
private eye	300	0.27	100000	98.23	79716.46	78.30	15095	14.81
qbert	161000	6.70	451900	18.82	580328.14	24.18	19091	0.79
riverraid	34076.4	3.28	36700	3.54	63318.67	6.21	17081	1.58
road runner	498660	24.47	128600	6.31	243025.8	11.92	57102	2.80
robotank	132.4	176.42	9.1	9.35	127.32	169.54	69.7	91.46
seaquest	999991.84	100.00	1000000	100.00	999997.63	100.00	2728	0.27
skiing	-29970.32	-93.10	-22977.9	-42.53	-4202.6	93.27	-9327	56.21
solaris	4198.4	2.69	4700	3.14	44199.93	38.99	3653	2.19
space invaders	55889	8.97	43400	6.96	48680.86	7.81	105810	17.00
star gunner	521728	200.00	414600	539.43	839573.53	200.00	358650	200.00
surround	9.96	101.84	-9.6	2.04	9.5	99.49	-9.8	1.02
tennis	24	106.70	10.2	75.89	23.84	106.34	23.7	106.03
time pilot	348932	200.00	344700	552.60	405425.31	200.00	150930	200.00
tutankham	393.64	7.11	191.1	3.34	2354.91	43.62	380.3	6.87
up n down	542918.8	200.00	620100	752.75	623805.73	200.00	907170	200.00
venture	1992	5.12	1700	4.37	2623.71	6.74	1969	5.06
video pinball	483569.72	0.54	965300	1.08	992340.74	1.11	673840	0.76
wizard of wor	133264	33.62	106200	26.76	157306.41	39.71	21325	5.26
yars revenge	918854.32	6.11	986000	6.55	998532.37	6.64	84684	0.54
zaxxon	181372	200.00	111100	132.75	249808.9	200.00	62133	74.22
MEAN SABER(%)		60.43		50.47		76.26		50.11
MEDIAN SABER(%)		33.62		21.19		43.62		13.90

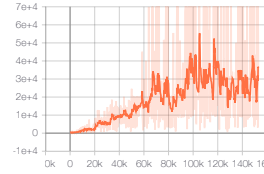
Table 5: Score table of SOTA 10B+ model-free algorithms on SABER.



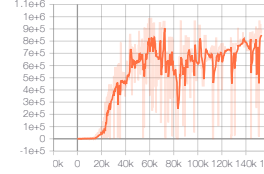
1. alien



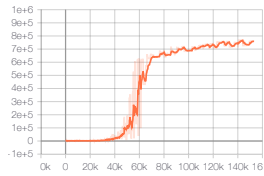
2. amidar



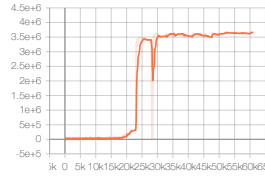
3. assault



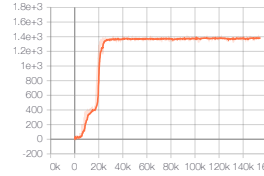
4. asterix



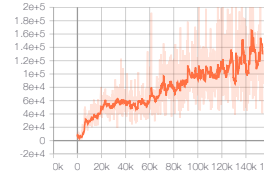
5. asteroids



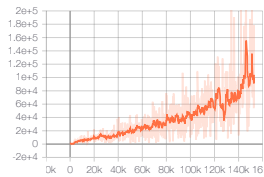
6. atlantis



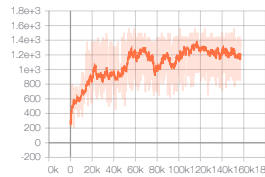
7. bank_heist



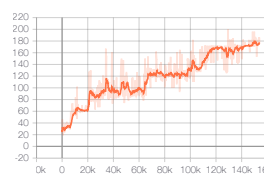
8. battle_zone



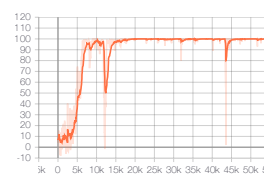
9. beam_rider



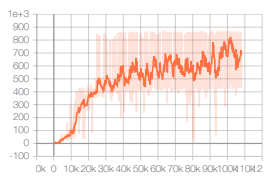
10. berzerk



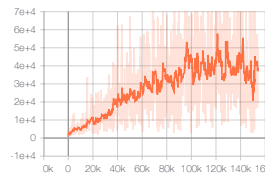
11. bowling



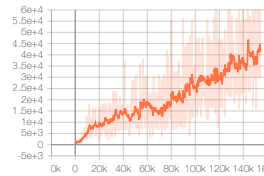
12. boxing



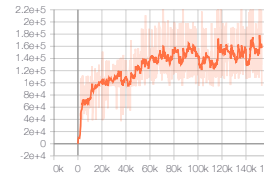
13. breakout



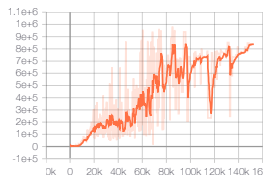
14. centipede



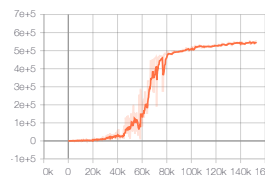
15. chopper_command



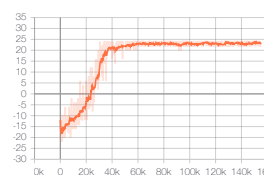
16. crazy_climber



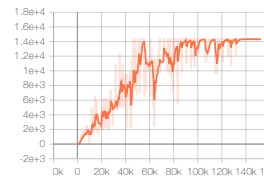
17. defender



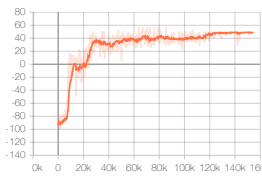
18. demon_attack



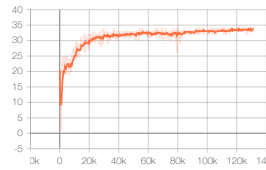
19. double_dunk



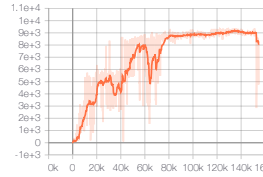
20. enduro



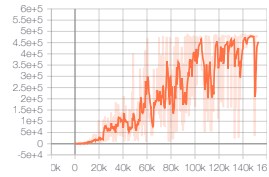
21. fishing_derby



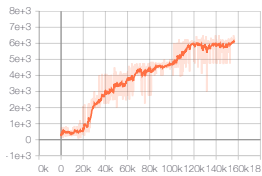
22. freeway



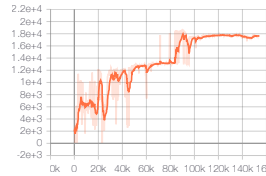
23. frostbite



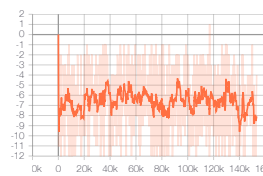
24. gopher



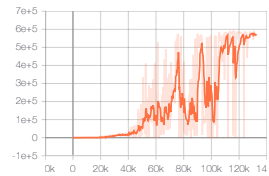
25. gravitar



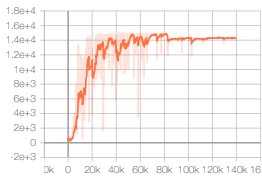
26. hero



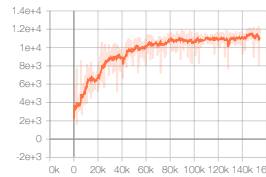
27. ice_hockey



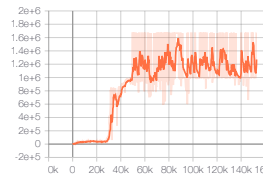
28. jamesbond



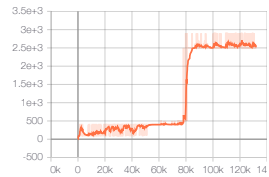
29. kangaroo



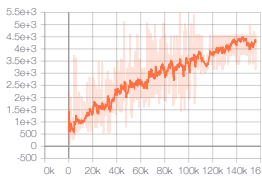
30. krull



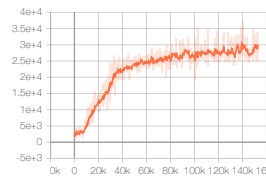
31. kung_fu_master



32. montezuma_revenge



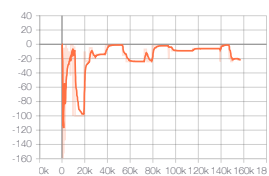
33. ms_pacman



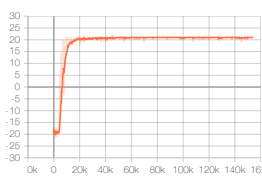
34. name_this_game



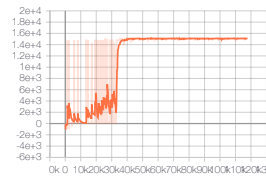
35. phoenix



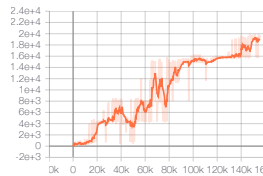
36. pitfall



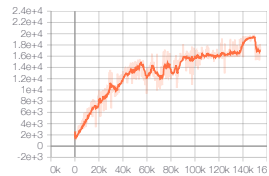
37. pong



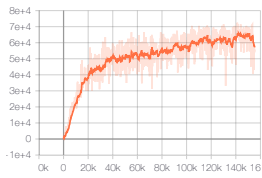
38. private_eye



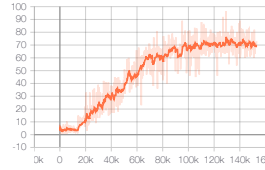
39. qbert



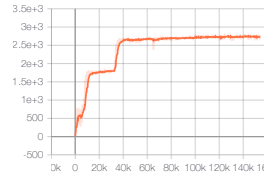
40. riverraider



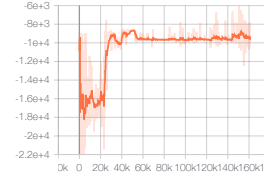
41. road_runner



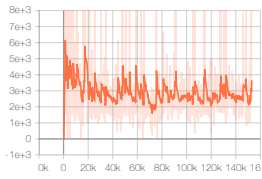
42. robotank



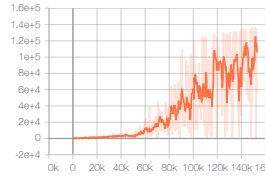
43. seaquest



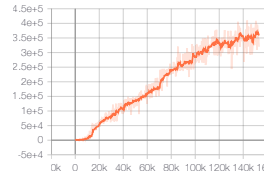
44. skiing



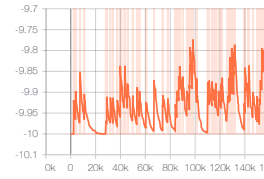
45. solaris



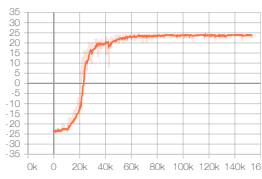
46. space_invader



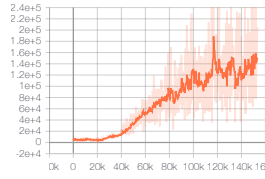
47. star_gunner



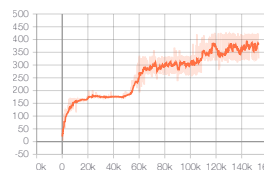
48. surround



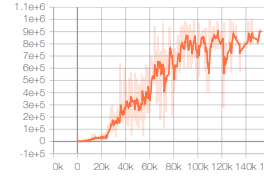
49. tennis



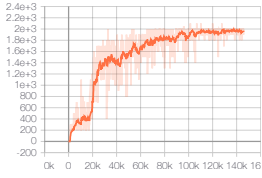
50. time_pilot



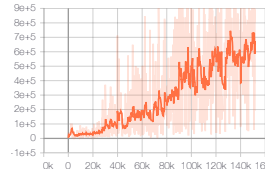
51. tutankham



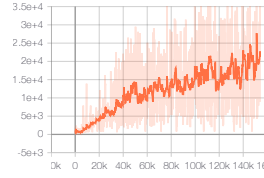
52. up_n_down



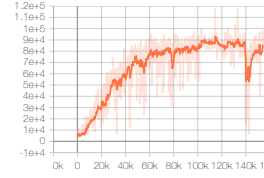
53. venture



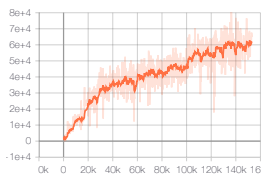
54. video_pinball



55. wizard_of_wor



56. yars_revenge



57. zaxxon